AN ABSTRACT OF THE THESIS OF

Yannick Duroy for the degree of Master of Science in
Geophysics presented on December 4, 1986.
Title: Subsurface Densities & Lithospheric Flexure of the Himalayan Foreland in
Pakistan Interpreted From Gravity Data

Abstract approved: _____ Signature redacted for privacy. _____

Robert J. Lillie

Gravity data along a N-S profile from Kohistan to the Punjab plain of Pakistan have been incorporated into recent interpretation of the gross structure of the foreland fold and thrust belt of the Himalaya. In northern Pakistan large deviations from Airy Isostatic equilibrium are observed. An excess of mass characterizes the northern Kohistan arc and a deficit of mass underlies a broad area extending from southern Kohistan to the Salt Range, while to the south a slight excess of mass seems to prevail in the region of the Sargodha ridge. This anomalous distribution of mass can be understood if the Indian elastic plate, which is assumed to overlie an inviscid fluid, is flexed down under the weight of both the overthrust mountains and the sediments eroded off the mountain and deposited in the foredeep basin. In many respects the intracontinental subduction of India beneath the Himalaya is similar to island arc formation, including the seismically active Sargodha ridge, an outer topographic rise analogous to the flexural bulge encountered seaward of oceanic trenches. Analysis of Bouguer gravity anomalies along a profile extending from the Sargodha ridge to the main mantle thrust (MMT) show that most of the negative-southward gravity gradient can be attributed to crustal thickening, while short wavelength anomalies are produced by lateral variation of density within the northward thickening sedimentary wedge. In the Sargodha ridge area, an additional contribution of about 25 mgals appears to be due to excess of mass at lower crustal or upper mantle levels. The Moho discontinuity is interpreted to bulge up beneath the Sargodha high, then gradually increase in dip from 1° to 3° beneath the Salt Range and Potwar Plateau (approximately equal to the change in dip of the basement surface). The Moho slope changes from upwardly convex to upwardly concave beneath southern Kohistan. Finally, north of the Main Mantle Thrust

(MMT) it bends down again, but at a steeper angle of about 15°. Shorter wavelength anomalies superimposed on the regional gradient are modeled in terms of upper crustal density changes, including those due to: 1) offsets of the basement surface, 2) variable thickness of the Eocambrian evaporite sequence that forms the basal decollement, 3) thrusting and folding of relatively high density, older parts of the stratigraphic section to higher structural levels, particularly in the Salt range and northern Potwar plateau, and 4) thickening of the low density Neogene molasse sequence into the axis of the Soan Syncline, a structural depression between the Salt range and northern Potwar plateau.

Subsurface densities of the overthrust wedge, as well as the definition of the shape of the top surface of the Indian plate interpreted from gravity, place bounds on the flexural rigidity of such a plate and the forces that deform it. In northern Pakistan the flexural rigidity of the elastic Indian plate ($D = 4.0 \times 10^{23}$ Nm) is a factor of 10 smaller than the current values interpreted for the central and eastern Himalaya. Because of the small elastic thickness interpreted for the Indian plate in Pakistan ($He \approx 30$ km), the Bouguer gravity gradient is steeper than in the Himalaya of India. Moreover the maximum flexural stresses are concentrated within the crust which may account for the seismic activity of the Sargodha ridge and southern Kohistan. At the end of the Indian elastic plate (arbitrarily chosen at the MMT), a large positive vertical shear stress, $S_0 = 9.2 \times 10^{12}$ N/m, is applied to account for the topographic load north of the MMT. In addition, to fit the gravity constraints it was necessary to apply a strong negative bending moment, $M_0 = -0.85 \times 10^{18}$ N, at the end of the plate. The negative bending moment is due to the combined effect of the northward migration of the Indian plate and the southward differential compressional force generated by the crustal rocks stacked beneath the northern Kohistan arc. Consequently, in southern Kohistan the surface of the Indian plate is concave. The upper portion of the elastic plate is therefore under compressional regime, while the lower portion is subject to extentional stress. High flexural stresses are probably the primary source of the Hazara seismic zone where incipient reverse faulting seems to take place. In contrast, the pronounced convexity developed along the flexural bulge can account for 1) tensional stress in the upper part of the Indian plate, large enough to produce basement normal faults interpreted beneath the Salt range and Sargodha ridge; and 2) compressional stress in the lower portion of the crust that cause the excess of mass and seismicity beneath the Sargodha Ridge.

Subsurface Densities & Lithospheric Flexure of the Himalayan Foreland in Pakistan,
Interpreted from Gravity Data

by

Yannick Duroy

A THESIS

submitted to

Oregon State University

in partial fulfillment of
the requirements for the
degree of

Master of Science

Completed December 4, 1986
Commencement June 1987

APPROVAL:

Signature redacted for privacy.

3/17/87
_____
Assistant Professor of Geophysics in charge of major

Signature redacted for privacy.   3-17-87
_____
Dean of College of Oceanography

Signature redacted for privacy.
_____
Dean of Graduate School

Date thesis is presented _____December 4, 1986_____
Typed by   _____Yannick Duroy_____

ACKNOWLEDGEMENTS

TABLE OF CONTENTS

LIST OF FIGURES

SUBSURFACE DENSITIES & LITHOSPHERIC FLEXURE OF THE HIMALAYAN FORELAND IN PAKISTAN INTERPRETED FROM GRAVITY DATA

INTRODUCTION

The ongoing collision between the Indian and the Asian crustal blocks is an example of the culmination of the Wilson cycle of ocean basin opening and closing. One consequence of this process is the creation of the Himalayan Ranges which extend westward from the Burma arc, through northern India, Nepal and southern Tibet, into northern Pakistan (figure 1). In Pakistan, the collision between India and Asia is recorded as a series of ENE-WSW trending structural zones, although to the south the Sargodha ridge trends NW-SE, parallel to major structures in the central Himalaya. Many features of the Pakistan Himalaya are similar to those of trench island arc systems but modified because light (Indian) continental crust is on the lower plate instead of oceanic crust. Surface geology, seismic reflection and gravity data show that the active foreland fold and thrust belt of Pakistan is analoguous in shape and dimension to accretionary wedges associated with subduction zones. The Sargodha ridge and its gravity signature are reminiscent of an outer topographic rise. Finally, the gravity data imply that the crust gradually thickens northward beneath the Kohistan arc (a wedge of island arc terrane trapped between the colliding Indian and Asian blocks; figures 2 and 3).

In this thesis previous observations, especially gravity anomalies are examined, in terms of subsurface densities in the foreland and lithospheric flexure along a Himalayan traverse in Pakistan. Analysis of the gravity field in the foreland thrust belt is emphasized because this area has been subject to intense geologic, seismic reflection and drilling investigations in the search for hydrocarbons (Khan et al., 1986; Lillie et al., in press) (figures 2 and 3), providing subsurface constraints for both gravity and flexural modeling. An analysis of gravity anomalies over the Sargodha ridge, as well as correlation with gravity studies undertaken in the hinterland by Marussi (1976) and Malinconico (1982,1986), provide further constraints on the
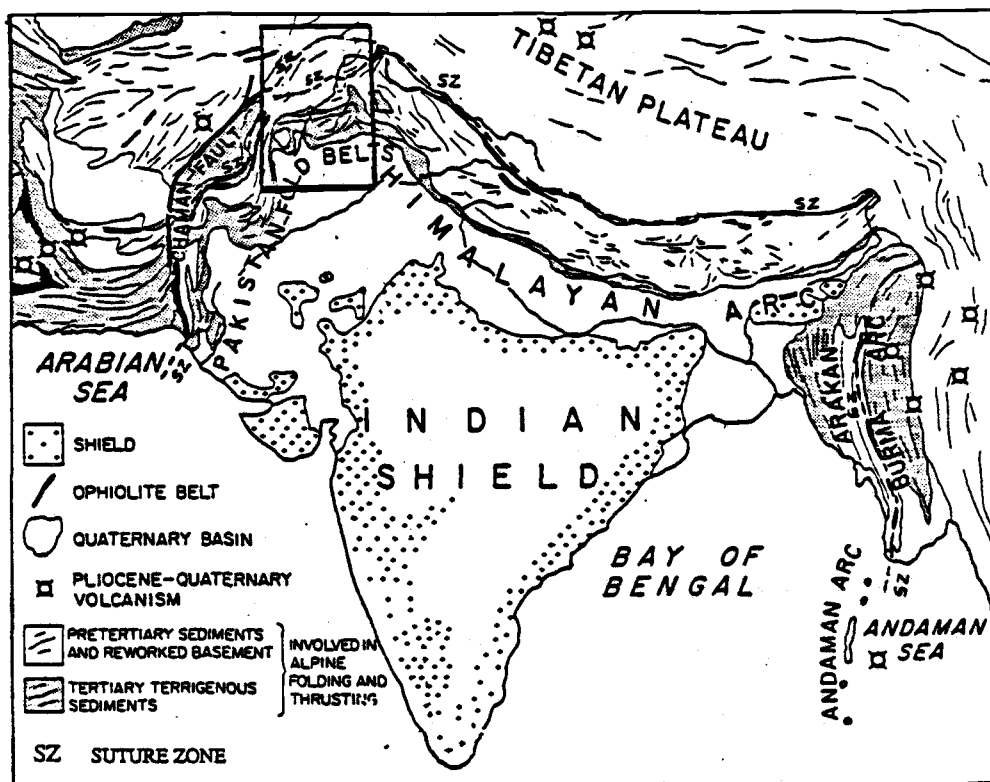
Figure 1 - Generalized tectonic map of the Himalaya. The location of the northern Pakistan map (figure 2) is indicated by the bold rectangle. After Seeber et al., 1981; based on Gansser, 1964.

Figure 2 - Generalized tectonic map of northern Pakistan, highlighting features in the Himalayan foreland. Seismic reflection coverage is within the areas of the two bold rectangles. Section A-A' is shown in figure 4. F-F' is line of section for lithospheric cross section (figure 3). Dotted lines north of Salt Range represent the two subsurface normal faults discussed in text. After Kazmi and Rana, 1982.
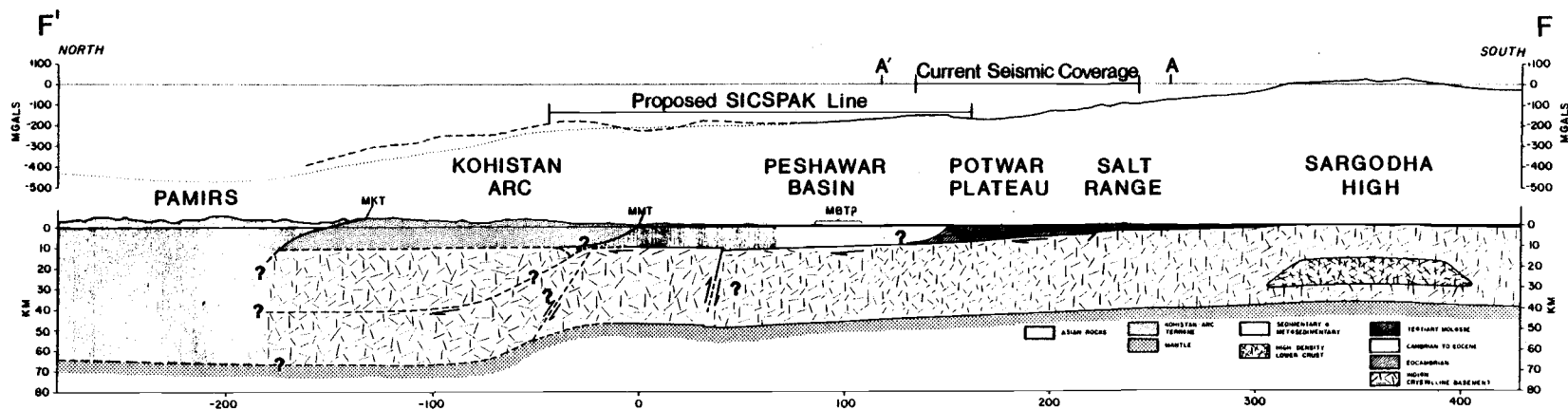
Figure 3 - Generalized cross section F-F' of the lithosphere from the stable Indian craton, across the Himalaya of Pakistan (see figure 2 for location). Bouguer gravity anomalies compiled from: a) km marks 277 to 427, Farah et al. (1977); b) km marks 77 to 277, Oil and Gas Development Corporation of Pakistan, published in Farah et al. (1977); c) dotted line, km marks -273 to 77, Marussi (1976); d) dashed line, km marks -158 to 77, is more detailed observations from Malinconico (1982, 1986), projected on to line of section. Gross upper crustal geometry of MMT and MKT from Malinconico (1982, 1986).

4

flexural model. The combination of the gravity and flexural analyses place additional constraints on the construction of balanced cross sections (Baker, Leathers and Pennock, in prep.) and mechanical models of the overthrusting in the foreland thrust belt (Jaumé, 1986). Furthermore, the flexural model provides an independent estimate of basement depth to check the velocity functions used to convert the seismic reflection profiles to depth. Ultimately, this study is an attempt to provide insight into several critical questions of lithospheric structure and evolution in the Himalaya of Pakistan:

1. How far to the north does the Indian plate behave elastically ?

2. Is the northern edge of the Indian elastic lithosphere free of or subject to any bending moment, vertical shear stress or compressional horizontal stress ?

3. Is the plate weaker beneath the Kohistan arc? If so, is it the northward transition from continental to oceanic lithosphere, or is it the result of a metamorphic front or other geologic process ?

4. Is it possible to correlate the stress distribution within the Indian elastic plate (as interpreted in the flexural analysis) with observed seismic activity ?

5. What is the origin of normal faults that offset the basement surface in the foreland of Pakistan ? Are they a response to ongoing flexure ? or are they older structures?

6. Is the Sargodha ridge really the expression of a lithospheric flexural bulge ? What causes the positive gravity closure observed in this area ? Was the ridge a positive topographic feature prior to Himalayan orogeny ?

TECTONIC AND GEOLOGICAL SETTING

The tectonic history of the Himalaya depicts the cycle of opening and closing of an ocean basin called the "Wilson cycle" by Dewey and Burke (1974). About 130 my ago an ocean basin (Thethys) lay between India and Eurasia as part of the Indian plate. Until approximately 40 to 55 my ago the oceanic portion of the Indian plate was consumed in a subduction zone at the southern margin of the Eurasian continent. Since that time the two continental masses have been colliding, resulting in a decrease in the rate of their convergence from 100 mm/yr to 50 mm/yr (e.g. figure 4 in Powell et al., 1973; Molnar et al., 1976; Yeats and Lawrence, 1985). The large thickness of low density continental crust has presumably inhibited the subduction of the Indian lithospheric plate resulting in the decrease in convergence rate; for this reason continued convergence of the two continental masses must be realized by processes other than subduction (Molnar, 1976). In addition to underthrusting of Indian basement beneath the foreland, crustal shortening along thrusts within the Himalaya and lateral movements of large blocks along strike slip faults in Asia account for this continued convergence between the Indian and Asian plates (Molnar et al., 1976).

In India the Indus suture is interpreted as the northwest-southeast boundary between the Indian and Asian continental blocks (figure 1). This east-west line of ophiolite melanges is the last remnant of the ocean floor that laid between them (e. g. Dewey and Bird, 1970; Gansser, 1964). North of the suture, rocks of igneous origin, similar to rocks of Andean-type margins, are encountered. South of the suture the rocks are crystalline rocks typical of the Indian plate.

The main India-Eurasia collision occured during the late Eocene. However, in the western Himalaya it was predated in late Cretaceous time by the docking of the Ladakh/Kohistan island arc complex with Asia (Tahirkheli et al., 1979; Windley, 1983). Beginning in the Oligocene, the Indian shield has been overriden by slices of its own northern margin which are stacked in a series of south-verging thrusts (Gansser, 1964). With increasing time these thrust sheets migrate southward over the Indian craton, forming new faults as movement of older ones slows and stops (Lefort, 1975; Mattauer, 1975). Erosion products from the thrusts are being shed into the

southward-migrating Siwalik molasse basin (Acharrya and Ray, 1982; Raiverman et al., 1983).

The Pakistan Himalaya can be divided into several major tectonic areas (Yeats and Lawrence, 1984; figures 2 and 3). These are from south to north: the Sargodha ridge, the Jhelum plain, the Salt Range, the Potwar and Kohat plateaus, the Hill Ranges, the intermontane basins, the southern Kohistan Ranges, the Nanga-Parbat-Haramosh massif, the Main Mantle Thrust (MMT), and the Kohistan island arc, which is separated from Asian rocks of the Pamirs to the north by the Main Karakorum Thrust (MKT).

In the Pakistan Himalayan foreland, the Precambrian crystalline basement is overlain by undeformed platform strata which are Eocambrian, Cambrian, Permian, Mesozoic and Cenozoic in age. Most of these strata are marine except for the late Cenozoic molasse associated with ongoing Himalayan collision. The seismically active Sargodha ridge (Seeber et al, 1979) is a basement high which runs parallel to the main trend of the central Himalaya (figure 2), and has probably been formed by late Cenozoic lithospheric flexure. The leading edge of the thrust system is expressed by the Salt Range (figures 2 and 3), where Phanerozoic strata override a décollement zone within Eocambrian evaporites (Salt Range formation; Crawford 1974). Movement along the base of the Salt Range (Salt Range thrust; figure 2) has occured in late Quaternary time (Yeats et al., 1984), but thrusting culminated 1.9 to 2.1 my. ago in the northern Potwar plateau (Johnson et al., 1979; Raynolds and Johnson, 1985). The northward transition from the Potwar plateau to the Hill Ranges (Kala chita, Margala hills) is along thrust contacts which may correspond to the Main Boundary Thrust (MBT) of India and Nepal (Yeats and Lawrence, 1984; Yeats and Hussain, in press). The Hill Ranges contain Precambrian slate, and Paleozoic, Cretaceous and lower Tertiary strata. The Peshawar and Campbellpur intermontane basins have been interpreted as the surface expression of the upper plate of low-angle detachement faults which ramp upward at the Hill Ranges (Yeats and Lawrence, 1984). To the north, the MMT juxtaposes crystalline rocks of the Kohistan ranges with the Kohistan islands arc terrane (figures 2 and 3). South of the MMT the Dargai klippe of ultramatic rocks seems to be a tectonic outlier of the MMT (Tahirkheli et al.,

1979).

       It appears that, generally, the different tectonic subdivisions in Pakistan do not correlate well with those of the Indian Himalaya; however some analogies can be identified between the two regions (Yeats and Lawrence, 1984): 1) the sub-Himalaya correlate with the Salt Range, Kohat and Potwar plateaus; 2) the Hill Ranges and southern Kohistan correspond to the lesser Himalaya; and 3) the Nanga-Parbat-Haramosh massif is equivalent to the high Himalaya.

PREVIOUS WORK

It was during the expedition of the French Academy to the Peruvian Andes (1735-1744) that Bouguer observed that there was a pronounced deficiency of mass beneath mountain ranges. However, the birth place of the theory of isostasy is probably the Himalayas. At the beginning of the 19th century, expeditions carried out by the Trigonometrical Survey of India resulted in observation that later led George Airy and John Henry Pratt to develop the ideas of isostatic compensation. Later; investigations made by differant groups of workers (Qureshy,1969; Qureshy et al., 1974; Kono, 1974; Choudury, 1975; Warsi et al, 1977; Mishra, 1982) led to the general agreement that the continental crust thickens northward beneath the Himalaya and Tibet. Wang et al., (1982) developed a 2-dimensional finite element model, suggesting that as the Indian plate underthrusts the Himalaya, the crust beneath Tibet thickens at a rate of 2 mm/yr.

In the two past decades the gravity field of northern Pakistan has also been analyzed by various workers. Regional Bouguer gravity and Airy compensation maps have been produced by Marussi (1976) for the Karakorum-Hindu Kush-Pamir region, mainly to study crustal thickness. The Geological Survey of Pakistasn (Farah et al., 1977) and the Oil and Gas Development Corporation (O.G.D.C.) have prepared Bouguer gravity anomaly maps of the Punjab plains, Salt Range and Potwar-Kohat plateaus (Khan et al., 1986). More recently Malinconico (1982, 1986) has made new gravity measurements across the Kohistan arc and its boundaries, to study the near surface structure of the arc and the structure of the crust beneath it.

Some other workers (Lyon-Caen and Molnar, 1983, 1985; Karner and Watts, 1983) have looked at the gravity field in the Himalaya from other points of view. They have shown that the gravity anomalies over the central Himalaya reflect anomalous mass distributions which can be interpreted in terms of lithospheric flexure. This thesis presents the first attempt to apply this type of analysis to the Himalaya of Pakistan.

METHODOLOGY

The purpose of this thesis is two-fold : 1) To refine previous interpretations of the gross density structure of the Pakistan foreland fold and thrust belt; and 2) to relate the interpreted density distribution to the flexure of the Indian lithospheric plate associated with Himalayan convergence in Pakistan. The first stage is a reinterpretation of the gravity field of the Himalayan foreland using gravity data published in Farah et al. (1977). A 130 km Bouguer anomaly profile running from the northern Potwar Plateau to the Jehlum plain (section A-A'; figures 2 and 3) is modeled using techniques developed by Talwani et al. (1959). The location of the gravity profile is purposely chosen perpendicular to the strike of major structural features, and through existing seismic reflection coverage. Surface geology and borehole data provide additional constraints. The second stage incorporates knowledge of the foreland in a plate tectonic framework, similar to the analysis of the Himalaya in India by Lyon-Caen and Molnar (1983-1985) and Karner and Watts (1983). The concept of lithospheric flexure at mountain ranges is derived from analogy to deflection of the subducting oceanic lithosphere at island arcs (Molnar, 1976; Lyon-Caen and Molnar, 1983). These areas are similar in the sense that much of the topography is supported by the bending of an elastic plate (Lyon-Caen and Molnar, 1983).

These concepts are applied to the Pakistan Himalaya to generate a flexural model from the MMT in the north, to the south of the Sargodha ridge. Basically this is an extention both north and south, of the gravity model generated in the first part of the thesis. The flexural model has to be consistent with the observed gravity anomalies; the main purpose of the flexural model is to improve the definition of the shape of the basement surface as well as of mass distribution in the foreland.

Based on an Airy isostatic anomaly map published by Marussi (1976), it has been suggested that in northern Pakistan there is an excess of mass beneath the Kohistan arc, whereas a mass deficit exists beneath the region from the Peshawar basin to the Salt Range. In the area of the Sargodha high, a slight exess of mass is observed.

It is assumed that the mass distribution results from the flexural response of an elastic plate (i.e. part of the continental lithosphere) to the distributed load of the Kohistan arc and southern Kohistan ranges. A model simulating this flexural response is developed, using gravity anomalies as well as the gross shape of the basement surface to place constraints on the mechanical properties of the plate and on the external forces that result in its deformation. Assuming elastic deformation is a simplistic approach which idealizes the behavior of the lithosphere. However, it is a reasonable assumption when a plate deforms with small curvature (Mc Adoo et al., 1978), which is the case for the continental lithosphere.

One way of analysing the bending of the Pakistan lithosphere is to consider a "truncated" Indian plate supporting part of the Himalayan load. The deflection of the Indian plate is only considered up to the MMT. The reason for applying this virtual truncation is that the deep crustal structure beneath the Kohistan arc (north of the MMT) is complex and not well constrained. It would probably be speculative to model the Indian plate beneath the Kohistan arc as a simple homogeneous elastic plate. Earthquake seismicity studies by Seeber (1979) and Menke (1976) demonstrate that the crust north of the MMT is highly deformed and faulted.Therefore a bending moment (M_0) and vertical shear stress (S_0) are applied at the end of the truncated Indian plate to account for the effect of external forces north of the MMT and the northern Kohistan arc load. Then in the flexural model the main topographic load is constituted by the southern Kohistan arc, the topographic load to the south up to the Salt Range is less significant.

This simple model helps to constrain the gravity interpretation in the foreland as well as the shape of the basement surface. It also provides an explanation for the Sargodha gravity high. Nevertheless the model does not give any information about how far the Indian plate underthrusts the northern Kohistan arc or the possibility that the plate is weaker beneath the northern Kohistan arc.

It should be noted that this model assumes plane stress and deformation. This might be a drawback in finding a realistic solution for the bending of the Indian plate in Pakistan. The physiographic expression of the Sargodha ridge reveals by its NW-SE direction, parallel to the overall Himalayan trend (figures 1 and 2), that there is

probably an important contribution of the central Himalaya to the Sargodha high. Therefore assuming two-dimensional plane stress and deformation is not an entirely satisfactory assumption. Unfortunately considering the three-dimensionality of the problem requires considerably more seismic reflection and other subsurface constraints than are currently available. The variables (mainly density contrast and depth to the basement surface in the foreland) would have to be closely defined at grid points of the flexural model for the solution to be more relevant than in the simple two-dimensional case.

It follows that the two-dimentional solution might be the most practical way to approach the problem of lithospheric flexure in the Pakistan Himalaya. Although the solution will bear some unquantifyable error inherent to the crude assumptions, it will provide a reasonable explanation to the gravity anomalies observed in the northwestern Himalayan thrust belt in Pakistan.

Establishing a flexural model requires the extension of the gravity model A-A' both north and south (section F-F') (see figures 2 and 3). Bouguer anomaly values for the area north of the Potwar Plateau are from Marussi (1976), as well as a projection of the observations by Malinconico (1986, personal comunication). South of the Salt Range, values are from the Bouguer gravity data published by Farah (1977).

GRAVITY MODELING

A.   Gravity data

The Bouguer anomaly in the Punjab plain of Pakistan is analysed along a NNW-SSE profile extending from 30 km south of the Salt Range to the Kalachitta Range, 100 km north of the Salt Range (section A-A', figures 2 and 3). The gravity profile is extracted from the Bouguer anomaly map produced by the Oil and Gas Development Corporation of Pakistan (O.G.D.C.) and published in Farah et al. (1977).

Because the Punjab plain is mainly constituted by young sedimentary rocks (Tertiary molasse), Farah et al. (1977) used a reduction density of 1.8 gm/cm^3 for the Bouguer correction. The maximum error for most of the Bouguer anomalies is estimated to be less than 3 mgals (Farah et al., 1977).

Using interpretations of subsurface structure from seismic reflection and drillhole data as constraints, the gravity data were modeled along section A-A', using the two-dimensional technique of Talwani et al. (1959).

In the second study, the previous gravity profile (A-A') is extended to the south (gravity profile A-F in figure 3), and to the north (gravity profile A'-F' in figure 3), to study the flexure of the lithosphere. The section to the south (A-F) is taken from the same Bouguer anomaly map prepared by Farah et al. (1977). Observed Bouguer anomalies obtained by Malinconico (1982), on a traverse running parallel to A'-F', but 30 km to the west, are projected along profile A'-F'. This part of the profile differs slightly from the portion to the south in that a reduction density of 2.67 gm/cm^3 was used to yield the simple Bouguer gravity anomaly.

The two sets of gravity data tie relatively well. For the segments F-A' and the projection of the Malinconico (1982) data, the ends tie within 2-3 mgals. Figure 3 also shows the observed Bouguer anomly profile (dotted line), derived from a Bouguer anomaly map with a 50 mgal contour interval, compiled by Marussi (1961). Those measurements were corrected using the 1930 standard gravity formula (as compared to the 1967 formula used for the other gravity data sets), and a reduction density of 2.67 gm/cm^3. The observed Bouguer anomaly agrees within 4-5 mgals with the observed

gravity of profile A-A'. Therefore, the gravity data from Marussi are used as a first order approximation for the flexural model.

B. Constraints

In northern Pakistan, the major structures are generally linear. Therefore, two-dimensional modeling is applicable.

Interpretation of gravity anomalies in the foreland is greatly facilitated by the extensive seismic reflection coverage. The seismic lines provide good control on the definition of the top of the crystalline basement. The interpretation of the seismic lines used to construct section A-A' (Lillie et al., in press; figure 4) provides the basic polygons representing gross structures within the overthrust section. Furthermore, seismic interval velocities, and lithologic description and density logs from wells, provide estimates for the subsurface densities used in the gravity model along cross sections A-A', and A-F. Nafe and Drake (1957) developed an empirical system of curves (published in Sheriff, 1984), relating seismic velocity to density for typical rocks. Applying these curves, Table 1 shows estimates of average subsurface densities for the different seismic units encountered in section A-A'.
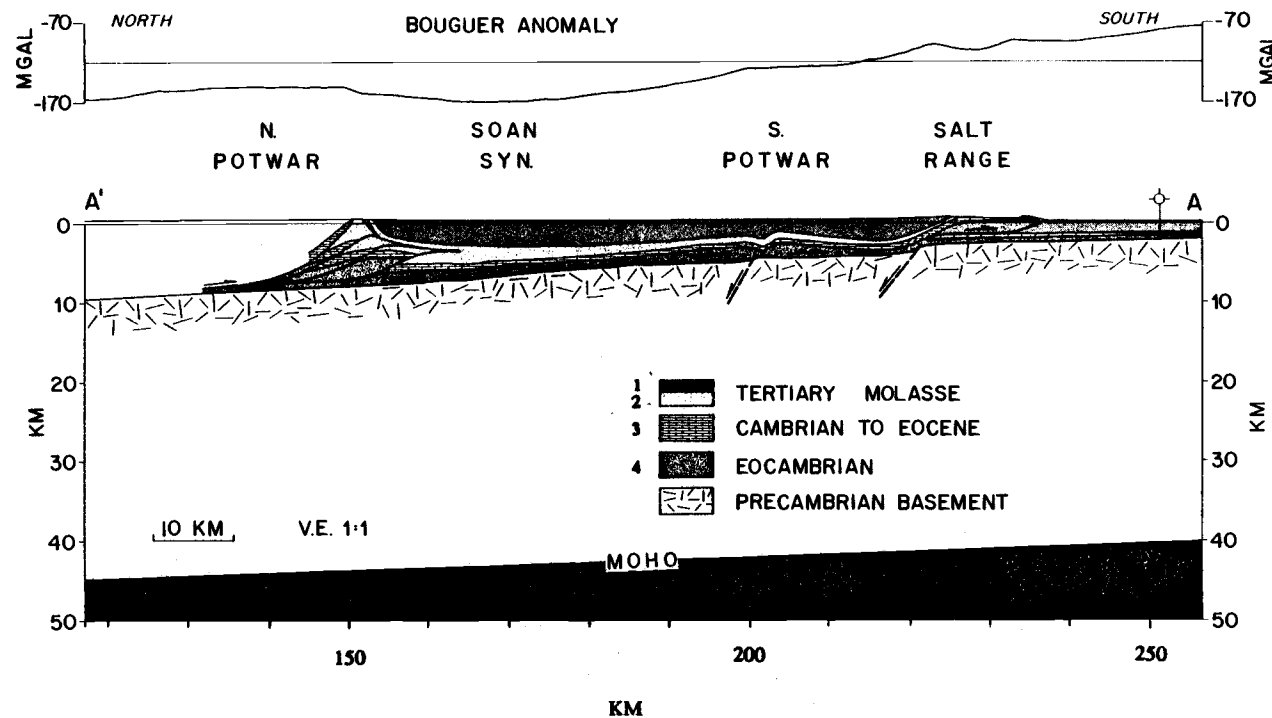
Figure 4 - Structural cross section and Bouguer gravity profile of northern Jhelum Plain, Salt Range and central Potwar Plateau (A-A'; figures 2 and 3). Section represents interpretation of four seismic lines, converted to depth (see Lillie et al., in press). Surface geology in Salt Range from Gee (1980), and in Potwar Plateau from O.G.D.C. Numbers on bottom of figure represent kilometer marks used as reference points in text. Numbers in stratigraphic legend correspond to seismic units listed in Table 1.

Table 1 - Estimated average densities of seismic units

Geologic Units	Seismic Units	Approximate Velocity (km/sec)	Approximate Density from Nafe-Drake curves (gm/cm^3)
Up. Siwaliks group	1a	2.3 - 2.5	
Molasse Mi. Siwaliks group	1b	2.9 - 3.0	2.1 - 2.4
section Lo. Siwaliks group	1c	3.3 - 3.7	
Rawalpindi group	2	3.4 - 3.8	2.3 - 2.5
Cambrian to Eocene compacted sediments	3	5.7 - 5.8	2.6 - 2.7
Eocambrian evaporite (Salt Range formation)	4	4.3 - 4.4	Approximation not valid because of low shear modulus of salt. Assumed 2.2 - 2.4

From the surface geology it is possible to place constraints on the upper polygons of the gravity model. In addition, the Shell number 1 Lilla well at km mark 251 (see figure 4) constrains thickness of the sedimentary layers south of the Salt Range. In this well Cambrian limestones are directly overlain by Siwalik molasse. The Permian, Eocene and Rawalpindi groups are absent.

Considering section A-F, no seismic line is available along this profile. However seismic velocities obtained for line A-A' help to constrain the densities of the sediments for the northern part of the Sargodha high. In addition, depth to basement maps derived from borehole and seismic reflection lines provide further constraints (e.g. figure 8 of Farah et al., 1977). Because of the flatness of the Punjab plain and the alluvium cover the bedrock geology of this area is not well documented.

The density of the Precambrian basement rocks (quartzite, and granitic gneiss) is generally assumed within the range 2.7 - 2.75 gm/cm^3 (Woolard, 1969; Farah et al., 1977; Malinconico, 1982). In northern Pakistan, Deep Seismic Soundings (DSS) carried out by Finetti et al., (1979), and Kaila (1981), short period earthquake seismic studies by Menke et al. (1976), as well as arrival times of compressional-waves from microearthquakes recorded by Roeker (1982), have yielded P-wave velocities of approximately 5.8 to 6.5 km/sec for the upper part of the crystalline crust. Kaila (1980) recorded P-wave velocities in the range 6.5 to 7 km/sec for the lower crust. According to the Nafe and Drake empirical curves, these velocities correspond to a density of approximately 2.65 to 2.8 gm/cm^3, for the upper crust and approximately 2.8 to 3 gm/cm^3 for the lower crust. Density contrasts at upper and lower crustal levels are relative to these values in the models shown in figures 5, 6 and 7. From the same seismic studies, P-wave velocities ranging from 8 km/sec to 8.2 km/sec suggest a density of 3.25 to 3.35 gm/cm^3 for the upper mantle. In the gravity models of the Pakistan foreland, we take a density contrast of 0.45 gm/cm3 between the lower crust and upper mantle. This value is close to the standard density contrast of 0.43 gm/cm^3 adopted by Worzel and Shurbet (1959) for continental section. We assume a value of 38 km for the thickness of the crystalline part of the crust beneath the craton as adopted by Kaila (1982) for the normal thickness of the crust under the Indian shield, which is assumed to be in isostatic equilibrium.

RESULTS OF GRAVITY MODELING

A.   Subhimalaya

The three figures 5a, 5b and 5c depict the analysis of Bouguer gravity anomalies in the Pakistan foreland along section A-A' (figures 2, 3 and 4). In the foreland thrust belt, the Bouguer gravity field follows an east-west trend (Farah et al., 1977). A general gradient of -0.75 mgal/km towards the north is interpreted in terms of the combined contribution of the deepening of the Moho and of the overall thickening of the overthrust wedge. Most of this gradient can be attributed to a northward dip of the Moho at roughly 2 degrees (figure 5a). With a density contrast of + 0.45 gm/cm^3 between the upper mantle and lower crust, a resulting regional gradient of -0.65 mgal/km towards the north is calculated. This is depicted in figure 5a by a decrease from -50 mgals to about -135 mgals from the northern Jehlum plain to the northern Potwar Plateau.

The residual gravity field labelled "sediment contribution" in figure 5b comprises shorter wavelength anomalies, which are an expression of density changes relative to the upper part of the basement.

Two normal faults, believed to be due to flexure of the lithosphere, offset the Precambrian crystalline basement. In the vicinity of these two faults, the gravity gradient steepens northward towards the downthrown fault blocks (km marks 199 and 221; figure 4). In the area of the Salt Range (km marks 217 to 237 in figure 4), the residual gravity field has a broad high of 15 mgals, which are interpreted as due to uplifted high density Paleozoic and Mesozoic strata (density contrast of only -0.05 gm/cm^3), combined with the effect of the large fault scarp. Superimposed on this gravity high is a shorter wavelength low with a maximum amplitude of -10 mgals (km marks 223 to 233). This feature is attributed to the thickening of the low density Eocambrian evaporite sequence beneath the center of the range. The average thickness of the salt core is estimated to be approximately 1.5 km, although the Dhariala well (drilled on the axis of a salt-cored anticline 20 km east of A-A') penetrated 2116 m of Salt Range formation (Gee, 1983).

Figure 5 - Density models of the Himalayan foreland thrust belt of Pakistan (section
A-A'; figures 3 and 4). (a) Regional Bouguer gradient can be modeled as due to
deepening of the Moho at a 2 degree angle northward. A density contrast of +0.45
gm/cm3 is assumed for the upper mantle vs. lower continental crust. (b) Shorter
wavelength Bouguer anomalies can be attributed to density contrasts at upper
crustal levels. Density contrasts are relative to the upper part of the basement. (c)
Models a and b added together result in a close fit between observed and calculated
Bouguer anomaly. There is no vertical exageration in the display of the models.
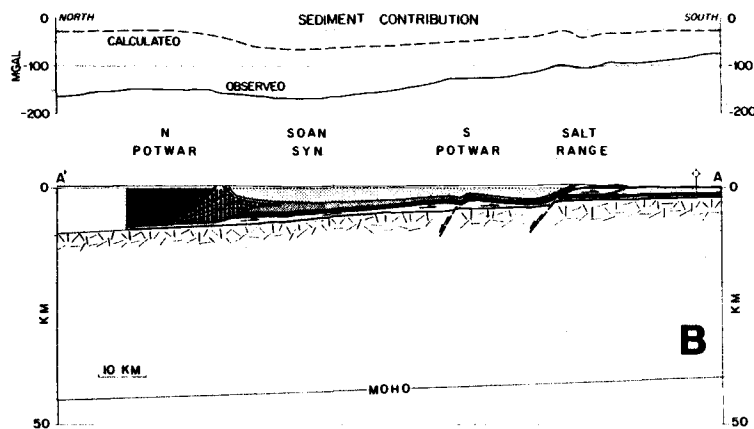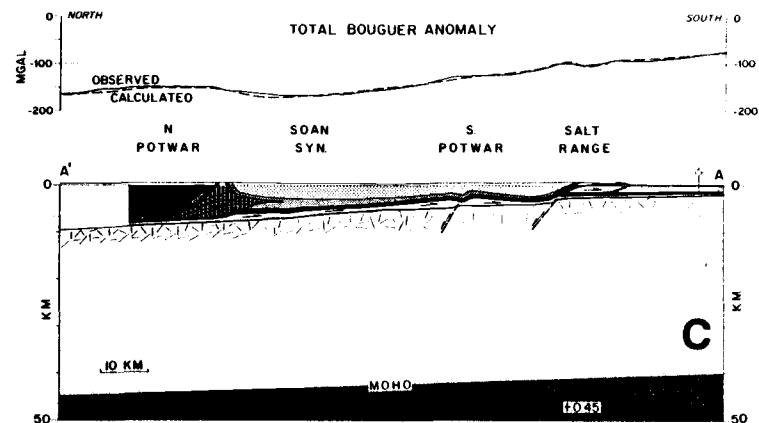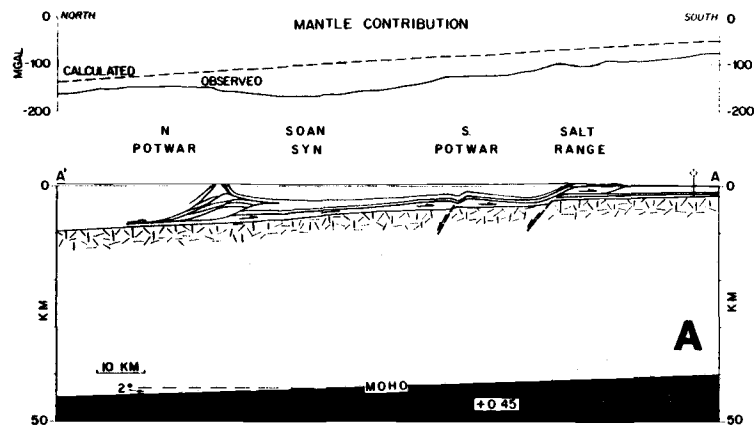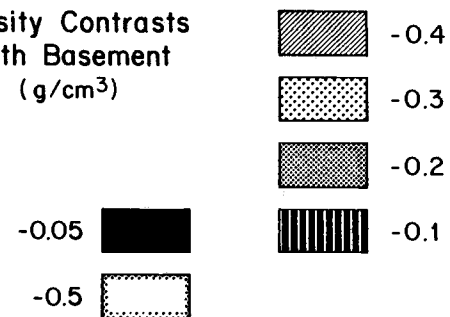
Figure 5

Farther north, the low density molasse sediments (density contrast of -0.3 gm/cm^3 for Siwaliks and -0.2 gm/cm^3 for Murees) are thickest (~ 5.5 km) at the axis of the Soan syncline (km mark 167). Consequently the residual Bouguer anomaly shows a broad low of approximately -50 mgals. On the north flank of the Soan syncline (km marks 142 to 154) an imbricate stack of thrust faults brings higher density (average density contrast of -0.10 gm/cm^3 relative to basement; +0.10 to +0.20 relative to molasse), Eocene and older rocks to higher structural positions, without involment of the basement (Lillie et al., in press). Therefore, the northward residual gravity gradient is interupted by a southward increase of +20 mgals. Although salt has been drilled by Occidental Oil in Dakhni field, the positive gravity anomaly suggests that there is not an appreciable thickness of salt within the imbricate stack; a portion 1/4 salt, 3/4 Cambrian to Eocene platform rocks is consistent with the observed gravity. Alternatively the salt might undergo a facies change from south to north; whereas almost pure salt rocks (density contrast - 0.5 to -0.45 gm/cm^3) are encountered in the area of the Salt Range, the Eocambrian Salt Range Fm within the imbricate stack (and perhaps farther north) may contain more clastics and is therefore of higher density (density contrast - 0.25 gm/cm^3). The interpretation of a facies change, together with the idea that the salt is probably pinching out north of the imbricate stack, is consistent with the observations that strata are highly deformed up to the imbricate stack but undeformed south of it (Jaumé, 1986; Jaumé and Lillie, in review). North of the imbricate stack the strata are more compacted and indurated, resulting in an increase of density (density contrast of only -0.05 gm/cm^3), which tends to flatten out the residual gravity gradient.

When combining the gravity contribution of the upper mantle with the gravity contribution of the sedimentary wedge (figure 5c), a close agreement between the observed and calculated Bouguer anomalies is achieved. The average deviation between the computed and observed anomaly is ± 3.0 mgals. This is reasonable considering the accuracy of ± 3.0 mgals in the determination of the observed Bouguer anomaly (Farah et al., 1977). Deviation from the observed profile may be partly attributed to an erroneous assumption in the Bouguer corrections assuming a constant density above the sea level datum. This assumption is especially not appropriate in the

Salt Range area, where formations such as compacted limestones and salt are thrust to the surface, providing a sharp lateral density contrast above the datum. Finaly,the simplicity of the crustal model does not result in high resolution. This is reflected in all cases (figure 5) by the calculated gravity profiles appearing much smoother than the observed gravity anomaly.

B.   Sargodha ridge

Figures 6a to 6e portray the analysis of the Bouguer gravity anomaly as observed in the area of the Sargodha ridge along profile A-F. The Bouguer anomaly of the Sargodha-Shah Kot ridge is expressed through a positive gravity closure with a NW-SE trend, almost parallel to the central Himalaya (see figure 2 of Warsi and Molnar, 1977)). In Pakistan this positive closure is flanked by a nearly north-south strip of decreasing gravity in the south and southwest and by a nearly east-west strip of decreasing gravity in the north. Profile A-F does not cross the Sargodha gravity anomaly at a right angle, but deviates 35 degrees to 40 degrees. However the approximation that the gravity model is perpendicular to the trend of the Sargodha ridge is made. The resulting gravity profile shows a boxcar shaped Bouguer anomaly between km marks +300 and +400. The amplitude of the closure is approximately 60 mgals with a peak Bouguer anomaly value of +27 mgals. Immediately to the north of the Sargodha ridge the gravity gradient is steep (-2 mgal/km), whereas to the south it dips more gently (-1.4mgal/km).

Farah et al. (1977) have attributed the prominent positive closures in the Sargodha-Shah Kot area to density contrast in the basement arising from igneous intrusions (dolerite, diabase). Although the possibility of these intrusions must not be ruled out, it was not possible to obtain a satisfactory fit to the positive gravity anomaly using this explanation. Therefore, an alternative explanation for the observed Bouguer anomaly over the Sargodha ridge is proposed.

The gravity field of the Sargodha-Shah kot ridge can be analyzed in term of the combined contribution of the basement topography, the lower crust, and the upper mantle in response to the flexure of the Indian plate. Using the Talwani (1959) method, it is possible to compute these three contributions (figures 6a, b and d).

Figure 6 - Density models of the Sargodha ridge of Pakistan (section A-F; figures 2 and
3). Bouguer gravity anomaly can be modeled as due to 3 contributions (a, b, and
d). (a) Basement topography. (b) Upward convexity of the upper mantle
attributed to flexural bending. The density contrast between the lower crust and
upper mantle is assumed to be +0.45 gm/cm3. (c) The misfit occurring without
the excess of mass within the lower crust. (d) An anomalous excess of mass of
+0.08 gm/cm3 within the lower crust, attributed to a phase change generated by
compressive flexural stress. (e) 3 contributions added give a close fit between the
observed and calculated Bouguer anomaly.
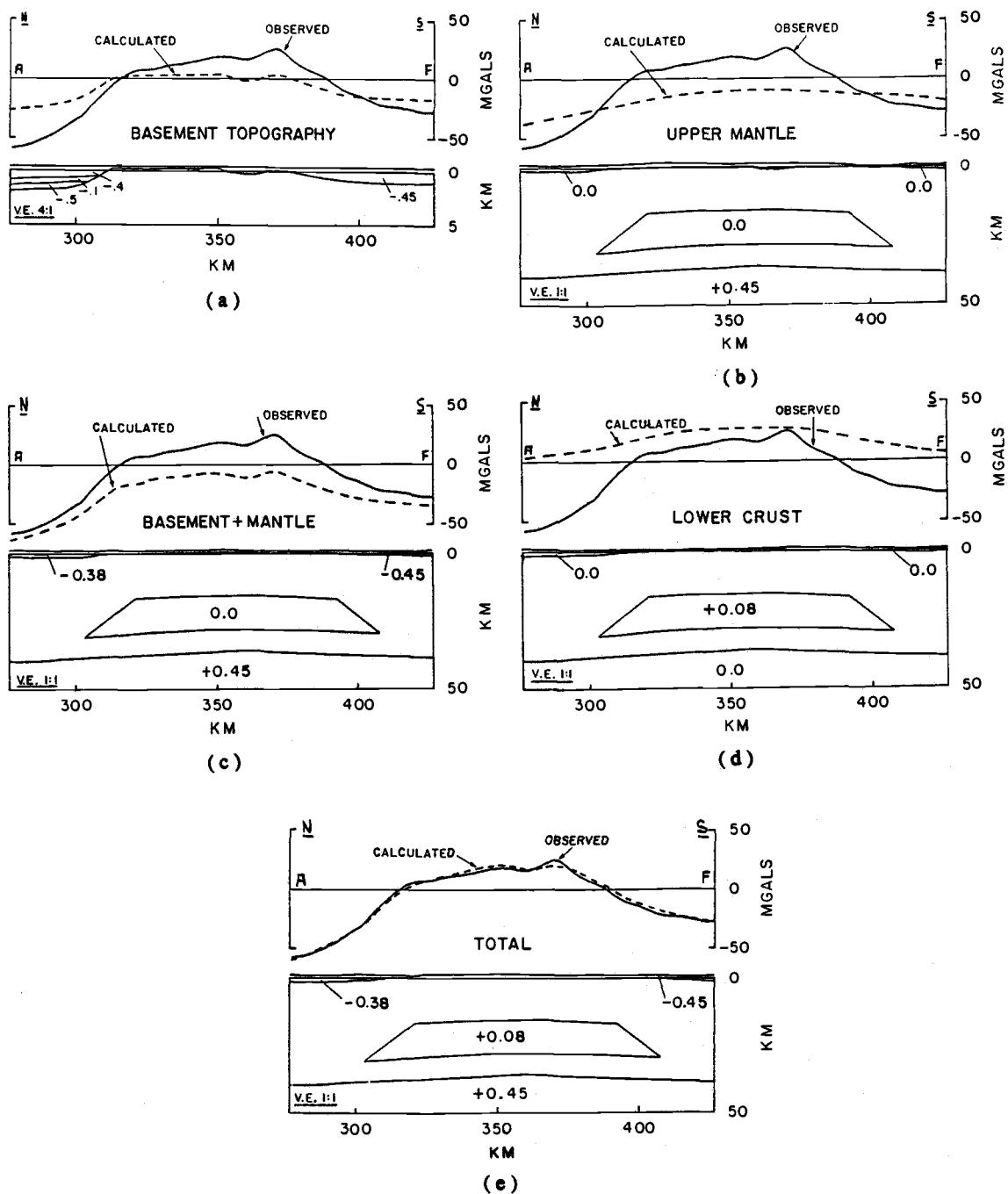
Figure 6

In figure 6a the gravity effect of the shape of the crystalline basement surface is computed. The topography of the top of the crystalline basement was constrained by depth to the basement map derived from seismic reflection lines (Leathers, Baker; in prep) and drill holes (Farah et al., 1977). In the area of the Sargodha high the crystalline basement is very shallow; outcrops occur within the Kirana hills. Along profile A-F the shape of the basement is tabular, and is perturbed by 2 major offsets at km mark + 305 to the north and km mark + 375 to the south. The northern offset may be interpreted as a normal fault due to lithospheric flexure; between km mark 310 and 300 the basement drops by about 1.5 km. The southern offset may be too gentle to be a normal fault, but instead may be an erosional feature. Because of these two discontinuities in the basement shape the sedimentary cover, which is as thin as 200 meters between km mark 310 and 375, increases drastically to 2 km thick to the north and 1.5 km to the south. The stratigraphic succession encountered in wells south of the Salt Range front (Eocambrian salt, Cambrian to Eocene platform sediment and Tertiary molasse) appears to be continuous until it reaches the normal fault interpreted to underly the north flank of the Sargodha ridge (figure 6a). South of the Sargodha ridge drill holes have penetrated the same strata suggesting that the Sargodha-Shah Kot ridge has been uplifted and erosion has scrapped off the sedimentary cover to leave a thin film of alluvium. The resulting gravity expression of the basement topography is a sharp boxcar shape like anomaly which closely mimics the short wavelength content of the observed Bouguer anomaly. The amplitude of the computed anomaly is approximately 20 mgals. The small gravity low between km mark 350 and 365 might be interpreted as an erosional channel carved in the crystalline basement by a stream or river.

Figure 6b displays the contribution of the upper mantle. The upward convexity due to flexure gives a mantle upward of 2km, which generates an anomaly of approximately + 16 mgals. Because the Moho dips about 2 degrees north of the Sargodha ridge but is flat south of it, the observed anomaly is slightly tilted to the north.

Figure 6c is intented to emphasize that the observed gravity anomaly along profile A-F is due not only to the sedimentary cover and mantle upwarp, but also to a

mass excess not accounted for in figures 6a and 6b. When the effects of the basement and mantle are added, the calculated anomaly is lower than that observed by approximately 25 mgals in the central part of the profile. Farah et al. (1977) also noted that an excess mass was required to fit the observed anomaly in the area of the Sargodha-shah kot ridge. They attributed this exess of mass to intrusive bodies of dolerite and diabase within the upper crust. It was not possible to model pofile A-F by this concept of igneous intrusions without coming up with geologically unreasonable dimensions for the intrusive body (e.g. sheeted dyke polygon 70 km x 2 km, with density contrast + 0.3 gm/cm^3). Therefore it is suggested that the excess of mass is at middle or lower crust levels.

Figure 6d shows the gravitational effect of an anomalous body of + 0.08 gm/cm^3 density contrast , within the lower crust. Later in the discussion, an explanation for the occurence of this body is given, which is consistent with the concept of lithospheric flexure and also geologically plausible. A density contrast of + 0.08 g/cm^3 was assigned to the lower crust polygon, so that it would account for the residual anomaly of figure 7c and still be geologically consistent. The shape of the polygon is the one which best fits the observed anomaly and the model of elastic flexure applied to the Indian plate. The resulting computed effect (figure 6d) is a broad "dome"-shaped positive anomaly of amplitude 23 mgals, with sharper wavelength than the upper mantle anomaly. It is also slightly tilted, but less so than for the upper mantle contribution.

By adding the gravity anomaly contributions (figure 6e), a close agreement between the computed and observed Bouguer anomalies is reached. The average difference between the calculated and observed anomalies is of ± 1.8 mgals.

The mass distrubution in the Pakistan Himalayan foreland is best explained in terms of lithospheric flexure. In its collision with Asia, the Indian plate is flexed downward creating a bulge which is typically expressed through the Bouguer anomaly as a broad high. It is suggested that the Sargodha high is the expression of such a flexural bulge. Because the bulge is an area of maximum curvature, it is where the maximun stress concentration occurs. In the case of upward convexity the elastic plate is under tensional stress above a neutral fiber, whereas it undergoes compression

beneath the neutral fiber. Earthquake seismic studies by Menke (1976), and Seeber and Armbruster (1979), have shown seismic activity within the crust in the area of the Sargodha ridge, down to depths of approximately 30 km. Tensional stress in the upper crust is probably responsible for the discontinuous shape (i.e normal faulting) of the basement surface in the Sargodha-shah kot and Salt Range/Potwar Plateau areas. If the elastic part of the Indian plate is confined within the crystalline crust (which is a conclusion given below in the second part of this study), then the lower crust must be in a state of compression in the region of the flexural bulge. Therefore it is suggested that the anomalous excess of mass required to fit the gravity anomaly along profile A-F is created by the compressive stress within the lower crust. As a matter of fact this concept is not new; Segawa and Tomoda (1976) interpreted positive residual gravity anomalies near the Japan and Izu-Bonin trenches in terms of a concentration of mass within a bending lithosphere, due to elastic compression, phase transformation, or magmatic flows.

Beneath the Sargodha Ridge the intensity of the compressive stress is large enough (maximum deviatoric compressive stress at the bottom of the elastic plate = 1.3 kbar) to induce cataclastic metamorphism. It is likely that a phase change occurs for some minerals due to the increase of tectonic pressure. For example the phase change sillimanite/kyanite (Ritsema et al., 1972) leads to an increase of specific density of $+0.4$ gm/cm^3 (Hurlbut et al., 1966). The phase change pyroxene granulite to garnet granulite (Hart et al., 1969) is a second example. In this case the specific density of minerals can be increased by $+0.5$ gm/cm^3 (Hurlbut et al., 1966). Both of these phase changes are reversible if the pressure decreases. Another possibility of phase change is the dehydratation of mafic or ultramafic minerals (for example the amphilbole to pyroxene phase transition) and can be expressed by an increase of specific density of $+0.3$ gm/cm^3 (Marty Fisk, personal communication). Finally, depending on the proportion of these minerals in the lower crust, the phase change might lead to an increase of density of $+ 0.08$ gm/cm^3 , as suggested by the gravity model (figures 6d and e).

Concerning the occurence of mafic or ultramafic minerals within the lower crust, it is possible that these minerals are present beneath the Sargodha-Shah Kot

area. Davis and Crawford (1971) have reported the exposure of dolerites and basic volcanics in the Kirana hills. Although these rocks (which have an isochron age of 870 ± 40 myrs) intrude into the upper crust, it is possible that the lower crust contains the gabbroic component of these basic rocks.

The anomalous excess of mass may no longer be present in the lower crust north of the Sargodha ridge. Therefore mafic minerals must undergo "retrometamorphism" by rehydratation, as the flexural bending stress is released north of the flexural bulge. It is important to mention that this rehydratation is only possible if the water is still available in the vicinity of the metamorphosed material, so that when the stress is gradually released this water migrates back to the reopening cracks and rehydrates the mafic minerals.

It should be mentioned that alternative explanations can account for the excess of mass underlying the Sargodha ridge; if there is a petrological change beneath the Sargodha ridge, or if the Moho discontinuity is brought up along 2 reverse faults. However modeling of the latter feature leads to a fit between the calculated and observed anomaly that is less satisfactory (i.e. the computed gravity profile has a slightly broader wavelength). If the Moho offset alternative is correct, then the Sargodha ridge may be the early stage of progression of crustal reverse faults through the foreland of the Indian plate (i.e. "incipient Main Central Thrust", see Yeats and Lawrence, 1984).

C. Section A'-MMT

Gravity profile A'-MMT was intended to put some additional constraints on the flexural model described in the second part of this study. Fom the Potwar plateau northward to the MMT, gravity data are taken from Marussi (1976); the results of the modeling are shown in figure 7. Although the calculated anomaly does not fit the observed as well as in the two previous models (average difference of ± 4.5 mgals), we can draw conclusions that help to constrain our flexural model. The most important result is that in southern Kohistan, the Indian plate changes from convex to concave upward. The top of the Indian crystalline basement reaches a maximum depth of 11.7 km at the location of a reverse fault interpreted to cut deeply into the

BOUGUER GRAVITY ANOMALY
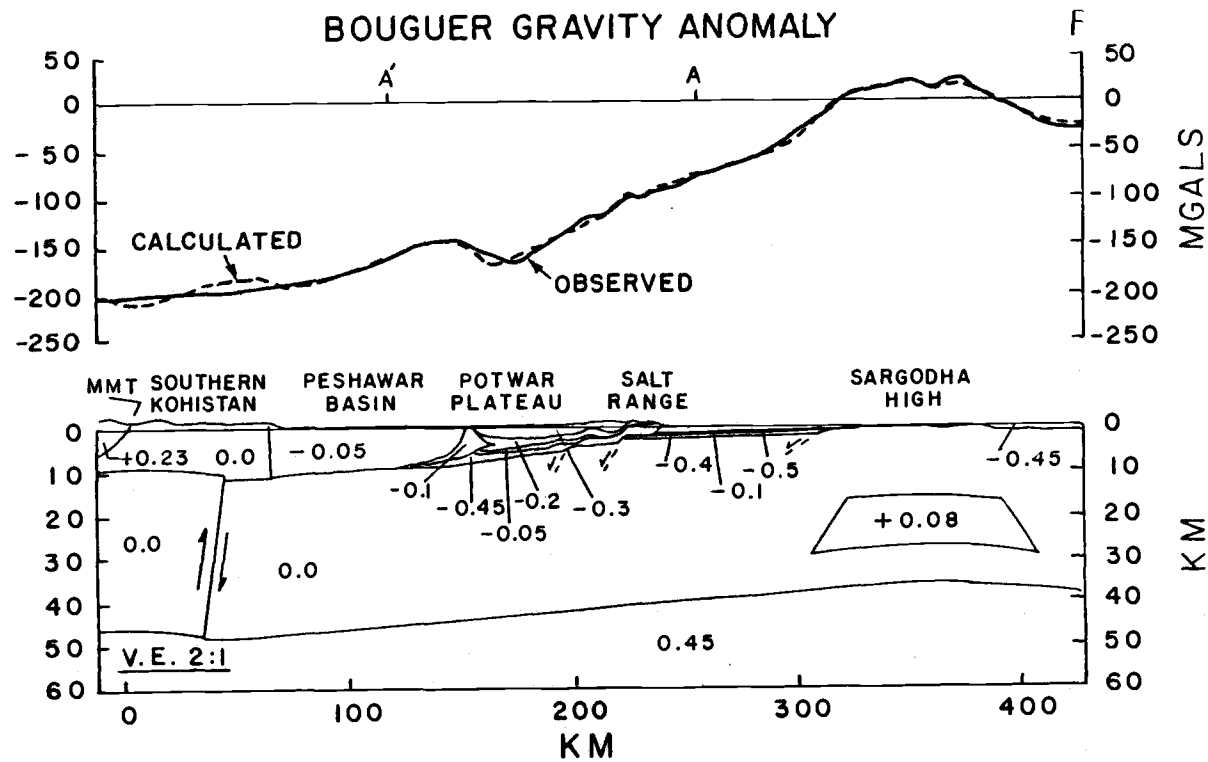
Figure 7 - Two-dimensional gravity model extending from the MMT to south of the Sargodha high. The subsurface densities and shape of the top surface of the Indian plate interpreted from this model are used as constraints in the flexural model. Sections A-A' and F-A are modeled in figures 5 and 6 respectively.

crust (km mark 40). North of the fault the basement surface slopes gently southward to reach 10.2 km depth beneath the MMT. The huge crustal reverse fault depicted in the gravity model was suggested by Seeber and Armbruster (1979) based on seismic activity recorded northeast of the Peshawar basin (Hazara Low Seimic Zone - HLZ). However, the gravity model disagrees with the crustal interpretation offered by Seeber in terms of the amplitude of the fault offset. It appears from the gravity that, if the crust is faulted, the offset is slight ($\approx$1km), compared to the 15 km of offset suggested by Seeber et al. (1979); there is no abrupt change in gravity that might suggest a 15 km offset of high density mantle material.

The gravity model also provides information about the densities within the overthrust wedge from the northern Potwar plateau to the MMT. The crustal rocks above the Indian plate are more indurated and deformed to the north, resulting in a northward increase of density. In southern Kohistan they reach a density similar to that of the crystalline basement.

Finally, from figure 7 it is possible to place some constraints on the flexural model. The shape of the basement surface is interpreted from the MMT to the south of the Sargodha high. Furthermore the density of the rocks above the Indian crystalline basement can be used as parameters in the flexural model discussed below.

It is important to emphasize that the overall shape of the basement surface in the foreland of Pakistan appears to follow the dip of the Moho (figures 3, 4, 5, 6 and 7), suggesting that there is little or no south-to-north thinning of the downgoing Indian continental crust. It therefore seems unlikely that the basement normal faults are associated with an earlier rifted margin of the Indian subcontinent. Instead, the overall upward convexity of the basement surface suggests that these faults probably resulted from lithospheric flexure during Cenozoic collision (Lillie and Yousuf, 1986). If crustal thinning of the Indian plate is preserved from an earlier rifted margin, it would have to occur somewhere north or northwest of the Potwar Plateau (Lillie et al., in press).

FLEXURE MODELING

A. Description of the flexural model.

The theory of linear elasticity is applied to the flexure of the Indian subcontinent in Pakistan, which is treated as a two-dimensional, thin plate. Although for section F-F' (figures 2 and 3) the two-dimensional approximation is not entirely valid (i.e. the Sargodha ridge is oriented NW-SE, parallel to the overall Himalayan trend but oblique to surficial structures in Pakistan), it is assumed that all major structures are linear and perpendicular to the direction of the section. The bending of such a plate under the load of the Himalaya and of the sediments that fill the resulting foreland trough is governed by the "biharmonic equation" (Turcotte and Schubert, 1982):

$$D \frac{\partial^4 W(x)}{\partial x^4} + g \Delta\rho(x) W(x) = Q(x)$$

where:

$W(x)$ = deflection of the plate at the abscissa x.

$Q(x)$ = weight/unit area of the topography at x.

$\Delta\rho(x)$ = density contrast between the 2 materials above and below the plate.

g = gravitational acceleration (assumed to be 9.8 m/sec^2).

D = $EH_e^3/12(1-v^2)$, flexural rigidity of the plate.

H_e = elastic thickness of the plate.

E = Young's modulus (assumed to be $\approx 1.6 \times 10^{11}$ N/m^2).

v = Poisson's ratio (assumed to be 0.25).

Note that in the biharmonic equation as described above, no horizontal compressive stress is considered.

The Indian lithospheric plate is assumed to overlie an inviscid fluid with a density corresponding to the material beneath the plate. That is, the underlying

material relaxes stress much more quickly than the elastic lithosphere. In addition to the topographic load, above the plate several segments are considered, with air, sediments and crustal rock densities.

As mentioned previously a flexural model extending from the MMT toward the south, is generated. Moreover the Indian plate is divided into five domains (figure 8) when solving equation (1) in order to approximate the mass distribution defined in the gravity model (figure 7). The five domains can be described as follows:

Domain 1 ($X0 < x < 60$)

This domain corresponds to southern Kohistan. It is the domain where the maximum topographic load is concentrated (figure 9). The load $Q(x)$ is considered to be the mass of rocks above sea level. $Q(x) = g \rho_1 T(x)$, where $T(x)$ is the thickness of material above sea level, calculated from the topographic profile, and ρ_1 is the mean density for the load (= ρ_{B1} = 2.7 gm/cm^3). The density contrast is $\Delta\rho(x) = \Delta\rho_1$ = $\rho_{B6} - \rho_{B1}$ where ρ_{B1} = 2.7 g/cm^3 (from gravity modeling) is the density of the crustal rocks above the plate and ρ_{B6} is the density of the material beneath the elastic plate.

Domain 2 ($60 < x < 150$)

It includes the area from the NE Peshawar basin to the northern Potwar Plateau. Here the topography is flat and lower than in the previous domain. $Q(x) = g \rho_1 T(x)$, where ρ_1 = ρ_{B2} = 2.65 g/cm^3. The density contrast is $\Delta\rho(x)$ = $\Delta\rho_2$ = $\rho_{B6} - \rho_{B2}$ where ρ_{B2} = 2.65 g/cm^3 (derived from gravity modeling).

Domain 3 ($150 < x < 240$)

This domain represents the area from the Northern Potwar Plateau to the southern front of the Salt Range. The topography is again low compared to the southern Kohistan and high Himalayas, but is enough to be considered as part of the topographic load (500 m < $T(x)$ < 1000 m). $Q(x) = g \rho_1 T(x)$ when ρ_1 = ρ_{B3} = 2.38

FLEXURAL MODEL
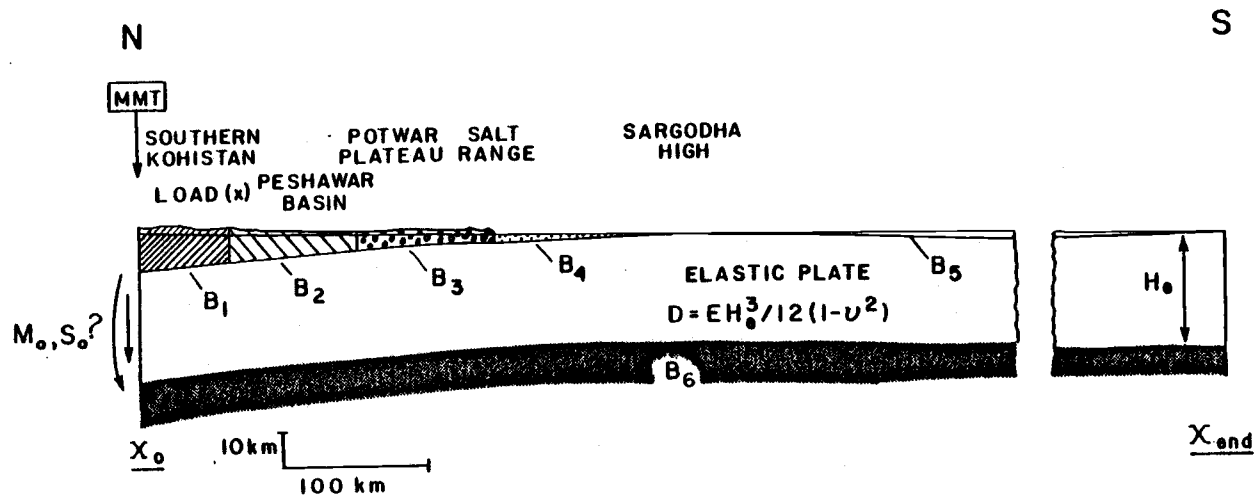
Figure 8 - Outline of the geometry of the numerical flexural model, applied to the
Himalayan fold and thrust belt in Pakistan. The geometry of the flexural model
attemps to approximate closely the gravity model discussed above (figure 7).
Above the Indian elastic plate 5 blocks (B1 to B5) represent the overthrust wedge
from the MMT to the south of the Sargodha ridge. Beneath the plate block B6
represents the buoyant viscous fluid. In addition to the topographic load $Q(x)$, a
bending moment M_0 and a shear stress S_0 applied at the truncated edge of the
Indian plate (Point X_0) account for the external forces and the topographic load
north of the MMT.

TOPOGRAPHY AND BASEMENT DEPTH
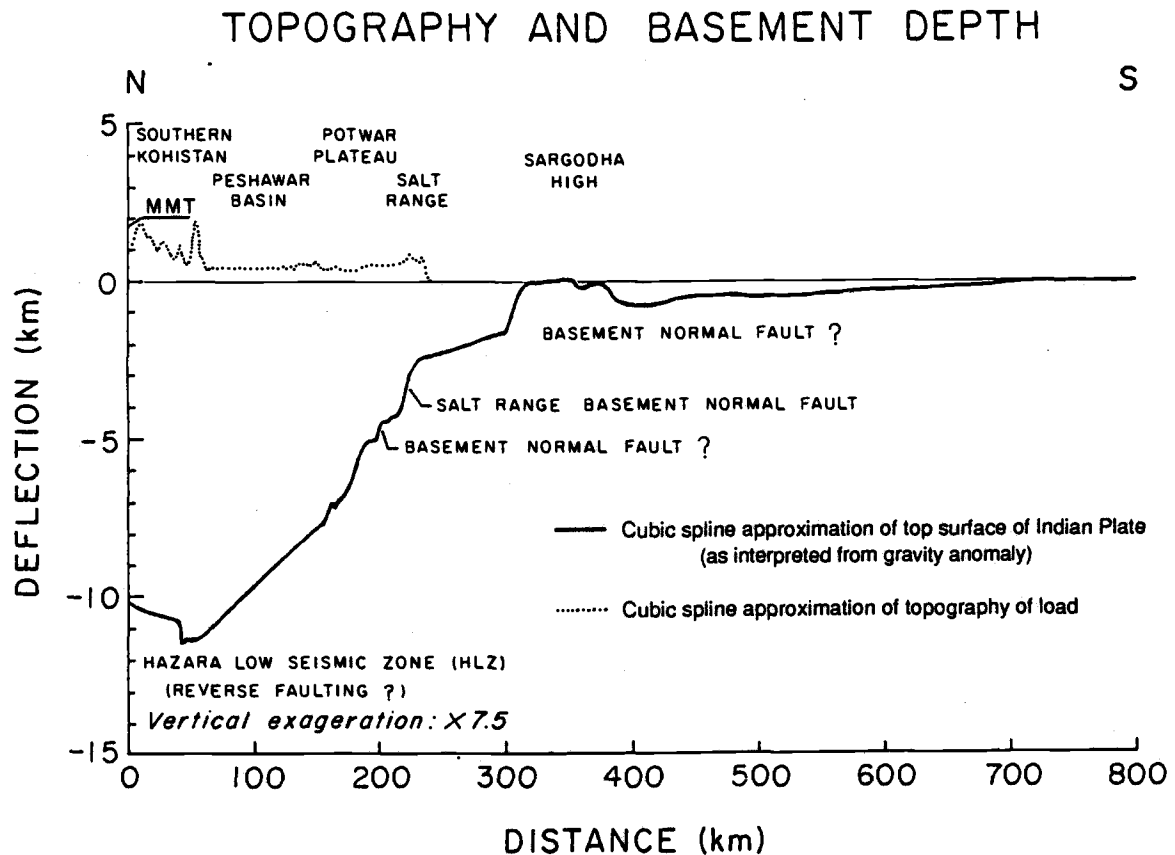
Figure 9 - Topography and basement depth from the Indian craton to the MMT in Pakistan (see figure 2 for location). Topographic load, as defined in flexural model of figure 8 extends from MMT to the Salt Range. The shape of the basement that we want to fit by the flexural model is interpreted from the Bouguer gravity data (figure 7).

g/cm^3. $\Delta\rho(x) = \Delta\rho_3 = \rho_{B6} - \rho_{B3}$ where $\rho_{B3} = 2.38\ g/cm^3$ (averaged density from gravity modeling).

Domain 4 (240 < x < 350)

In this domain, extending from south of the Salt range to the Sargodha Ridge, the topography is very low (less than 400 meters) and is therefore assumed to be insignificant. Then $Q(x) = 0$, and Equation (1) is said to be homogeneous. The density contrast $\Delta\rho(x) = \Delta\rho_4 = \rho_{B6} - \rho_{B4}$ where $\rho_{B4} = 2.32\ g/cm^3$ (average density derived from gravity modeling).

Domain 5 (350 < x < Xend)

It includes the area of the Indian shield from the Sargodha Ridge southward. In this case equation (1) is also solved with $Q(x) = 0$. The density contrast is $\Delta\rho(x) = \Delta\rho_5 = \rho_{B6} - \rho_{B5}$ where $\rho_{B5} = 1.8\ g/cm^3$. ρ_{B5} was not determined from the gravity model but assumed, considering that it is the density of the molasse and alluvium sediment that were deposited above the Indian plate following its collision with Asia (see Farah et al., 1977). In other words one can consider that in this domain the sedimentary rocks deposited on top of the Indian plate prior to collision are part of the elastic Indian plate.

Now we must seek a solution for the deflection of the Indian elastic plate that fits the solution obtained for the basement surface shape from the gravity model (figures 7 and 9). To solve the biharmonic equation a program called "Flexdur", based on a finite difference method was designed (see Appendices 1 and 2).

The topographic load and density of the material above the plate are defined as stated above for domains 1 through 5. It remains to specify the Bending moment (M_0) and the vertical shear stress (S_0) at point X_0 to account for the effect of the load applied north of the MMT (figure 8). In addition, we have to assign an appropriate flexural rigidity D. This latter variable also puts some constraints on the specification of the density of the material beneath the plate (ρ_{B6}). Indeed, given the Young's modulus E and a Poisson's ratio for the Indian plate, the flexural rigidity is directly

related to the elastic thickness H_e of the plate. For a chosen flexural rigidity there will be a particular density appropriate for the material beneath the plate (only mantle material for thick plates, possibly lower crustal in addition to mantle material for thinner plates).

B. Interpretation - Discussion of the results.

The approach to the problem of fexural modeling of the Himalayan foreland in Pakistan is dependant on the nature of the constraints available in this region. Because of the seismic reflection coverage in the foreland, as well as drill holes and surface geology, the gravity modeling of the area was well constrained. Therefore, the gravity model along profiles A-A'(figure 5) and the Sargodha Ridge (figure 6) provide reliable constraints for flexural modeling. The mass distribution within the entire overthrust wedge is estimated from additional gravity modeling (figure 7), and is approximated in the flexural model (figure 8) by 5 blocks (B1 to B5) overlying the Indian plate. Flexural modeling is performed with the main purpose of matching as closely as possible the shape of the top surface of the Indian plate as interpreted from gravity data (figures 7 and 9). The topographic load and the densities of the rocks above the elastic plate are assumed from considerations of the nature of rocks exposed at the surface and from the gravity modeling (figures 5, 6, and 7). The density of the material beneath the elastic plate (block B6) is assigned depending on the elastic thickness of the plate. Performing flexural modeling is now a matter of finding the mechanical properties of the elastic plate and the forces that deform it. In other words, 3 unknown variables remain to be determined: 1) the flexural rigidity D of the elastic Indian lithosphere, 2) the bending moment M_0 applied at X_0, and 3) the vertical shear stress S_0 applied at X_0. Although these 3 parameters are unknown, they must lie within certain ranges imposed by rock mechanics. The buoyancy force also has a noticeable effect, but because it appears through the choice of density of the material beneath the elastic plate, it is connected to the choice of flexural rigidity.

Several series of calculations were performed for a variety of assumed values for the flexural rigidity, bending moment M_0 and vertical shear stress S_0 to come up with a satisfactory solution (figure 10).
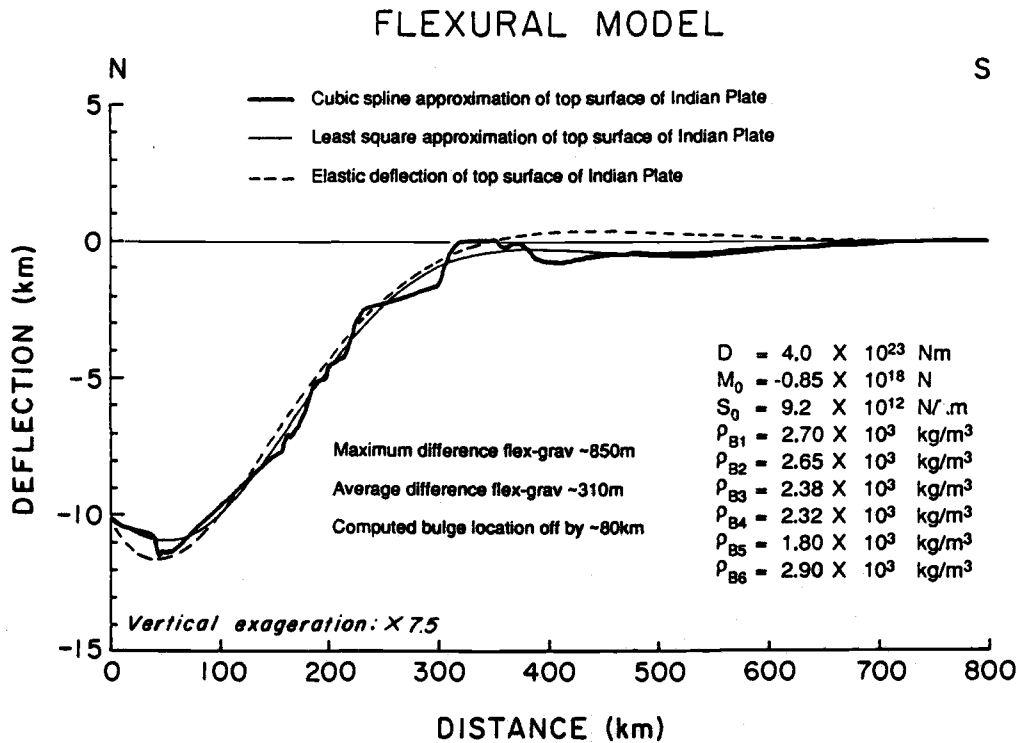
Figure 10 - Shape of the top surface of the Indian plate inferred from gravity model (figure 7). Heavy line = rough shape, light line = smoothed shape. The solution for the shape of the top surface of the Indian plate computed in the flexural model is displayed as a dashed line. ρ_{B1} to ρ_{B6} represent the densities of the 6 blocks of the flexural model (figure 8), as interpreted by gravity modeling (figure 7). The flexural rigidity D, the bending moment M_0 and the vertical shear stress S_0 are the 3 variables that were modeled in order to approximate the basement surface configuration.

The three profiles plotted in figure 10 represent the top surface of the Indian plate from the MMT to the south of the Sargodha ridge. The plain line represents a cubic spline approximation of the basement surface interpreted from the Bouguer gravity anomaly (same as in figure 9). The main features (such as the Sargodha ridge, the basement normal faults, and the Hazara reverse fault) are emphasized due to the vertical exaggeration of 7.5:1. The light line represents a least square smoothing of the cubic spline representing the shape of the top of the Indian plate. It is this smoothed curve that is modeled through the flexural analysis. The dashed line represents what is considered the best solution for the elastic deflection of the Indian plate. The maximum difference between the flexural solution and the least square approximation is 850 meters (at km mark 450); whereas the difference is 300 meters between km marks (100 and 300). The most significant misfit is probably the offset of the location of the computed flexural bulge which was calculated 80 km south of the observed bulge, namely the Sargodha ridge. The computed height of the flexural bulge (370 meters above sea level) seems to be a reasonable value considering the elevation reached in this vicinity (Kirana Hills $\approx$ 500 meters above sea level). Later in the discussion some ways of improving the solution are suggested, but for this study the accuracy reached in the model is probably good enough to illustrate the concept of flexure applied to the foreland of Pakistan.

The calculation showed that the flexural rigidity is the major factor controlling the dip of the elastic plate, the width of the foredeep basin and the position of the flexural bulge, as well as its height. Constrained by the range of values currently used by various authors (e.g. Lyon-Caen and Molnar; 1983, 1985) for the flexural rigidity of the Indian plate, several computations were performed. The flexural rigidity of the Indian plate for the area of the Pakistan Himalaya appears to be relatively small: $D = 4.0 \times 10^{23}$ Nm. However, this value tends to support the observation made by Lyon-Caen and Molnar (1983, 1985) and Karner and Watts (1983) concerning the values of flexural rigidities along the central Himalayan Arc. These authors suggested that the flexural rigidity for the westernmost part (i.e. toward Pakistan) seems to be from 3 to more than 10 times smaller than that determined in the central or eastern part of the range. Whereas values for D between 2.0×10^{24} and 2.0×10^{25} Nm were

found in the central and eastern parts, it seems that for the northwestern part of the Himalaya the flexural rigidity decreases dramatically to values between 2.0×10^{23} Nm to 1.0×10^{24} Nm. Differences in the gravity field are also apparent. On the Bouguer anamoly map (see figure 2 of Warsi, 1979) the gravity gradient is much steeper west of longitude 78° E and north of latitude 28° N.

The relatively small flexural rigidity of the Indian plate in Pakistan implies a small equivalent elastic thickness. Since $D = EHe^3 /12(1 - v^2) = 4.0 \times 10^{23}$ Nm, the corresponding elastic thickness H_e is approximately 30 km, given Young's modulus $E = 1.6 \times 10^{11}$ N/m and Poisson's ratio $v = 0.25$. Therefore, the elastic portion of the Indian plate is confined within the crystalline crust whose total thickness is assumed to be 38 km. A direct implication is that the lower crust acts as part of the buoyant fluid supporting the elastic Indian plate. This is made possible if the lower crust has a ductile behavior, as is generally believed. A density of 2.9 g/cm^3 has been used for the buoyant fluid beneath the elastic plate. The buoyancy force $g\Delta\rho(x)W(x)$ acting on the plate is considerably reduced compared to what it must be for the larger elastic thickness encountered in other parts of the Himalaya. For elastic thickness greater than the crustal thickness, only mantle material acts as the buoyant fluid. The average density contrast between material above and beneath the plate is approximately 1 g/cm^3 when only mantle is underlying the plate; it is only about 0.6 g/cm^3 in the Pakistan foreland where the lower crust acts as part of the buoyant material. Therefore, beside the fact that the flexural rigidity is small in Pakistan, the small buoyancy force allows the plate to bend even more sharply than it would bend if the upper mantle alone would be the buoyant fluid. However it was possible to obtain a similar solution assuming a density of 3.3 gm/cm^3 for the material underlying the elastic plate. With this density the flexural rigidity of the plate appears to be slightly larger ($D = 6.0 \times 10^{23}$ Nm, corresponding to an elastic thickness $H_e = 35$ km); however, it was necessary to apply extremely large bending moment and vertical shear stress ($M_0 = -1.4 \times 10^{18}$ N, $S_0 = 1.62 \times 10^{13}$ N/m).

In addition to the topographic load distributed from the MMT to the Salt Range, the inclusion of a bending moment M_0 and vertical shear stress S_0 is required to account for external forces applied at the end of the truncated Indian plate. To

account for the negative curvature interpreted between km marks 0 and +100, a negative bending moment $M_0 = - 0.85 \times 10^{18}$ N is applied at point X_0. Moreover, it was necessary to apply a large moment in order to bring the elastic solution towards the shape of the plate interpreted from the gravity data. Without this large bending moment the dip of the plate is too large (by a factor of 2 in the case of no bending moment); the bulge has too high an amplitude and is located north of where it actually occurs (Sargodha Ridge). The existence of such a large negative bending moment can be attributed to the buttress effect created by the crustal blocks stacked beneath the Kohistan arc (Malinconico, 1982,1986; Malinconico and Adams, 1986). As the buoyant crust of the Indian plate underthrusts Asia, it undergoes a strong horizontal opposition on its upper part from crustal slices stacked under the Kohistan arc. The net effect of this collision is equivalent to a negative bending moment that elevates the northern end of the plate and in reaction depresses a portion farther south.

The large topographic load constituted by the northern Kohistan arc also contributes to the deflection of the Indian plate. Its contribution is approximated by a large positive vertical shear stress applied at X_0. To bring the end of the "truncated" Indian plate to the depth interpreted from the gravity anomaly, it was necessary to include a large vertical shear stress S_0 with a magnitude of 9.2×10^{12} N/m.

Because of the tremendous stresses which are interacting in the area of the Kohistan arc, high seismic activity is recorded in this region down to depths of tens of kilometers (Seeber et al., 1977). Bending of the Indian elastic plate generates large stresses in the area of great curvature. For the complete elastic behavior model the bending moment is directly related to the curvature and the flexural rigidity $M = - D (\partial^2 W / \partial x^2)$. From this, one can estimate the deviatoric stress produced inside the elastic plate at any depth above or below the neutral fiber. The deviatoric stress is given by $\sigma_x = 12 \, MZ/H_e^3$ (Mc Adoo et al., 1978), where Z is the vertical coordinate whose origin (Z = 0) is taken at the neutral fiber. One can use this to calculate the "compressive" deviatoric stress produced by the flexural bending at the base of the elastic plate in the area of the Sargodha ridge. From the least square approximation of the top surface of the Indian plate we can approximate the curvature of the Indian plate at the Sargodha ridge as: $\partial^2 W / \partial x^2 = - 0.5 \times 10^{-7}$ m^{-1}. This gives a

bending moment: $M = - D (\partial^2 W/\partial x^2) = - 4.0 \times 10^{23}$ Nm $x - 0.5 \times 10^{-7}$ m^{-1}
$= 2.0 \times 10^{16}$ N. The maximum absolute value of the deviatoric stress produced by this
bending moment occurs at the bottom and the top of the elastic plate and is given by
$| \sigma_x | = (12 \times 2 \times 10^{16} \times 30 \times 10^3 /2)/(30 \times 10^3)^3 = 0.13 \times 10^9$ N/m^2 = 1.3 kbar.

The actual tensile strength of rocks as observed in laboratory experiments is
less than 1 kbar at low confining pressure (see figure 3 of Bird, 1978; and figure 2 of
Karner et al. 1983). Since $| \sigma_x | > 1$ kbar, we can expect a brittle failure of the top
surface of the Indian plate in the foreland due to bending tensional stress. Indeed, this
is what is happening, as normal faults are observed to offset the crystalline basement
in the Salt Range and Sargodha ridge area. Similar normal faults have been interpreted
in earthquake focal mechanism studies of the Ganges Basin and Subhimalaya of India
by Molnar et al. (1976) and Ni and Barazangi (1984). Seismic activity is also
recorded in the area of the Sargodha ridge within the upper and mid crust (see figure 9
of Seeber and Armbruster, 1979). Concerning the bottom of the elastic plate, which is
within the compressional regime, the excessive deviatoric stress of 1.3 kbar may
induce rock failure, despite the hydrostatic pressure at this depth (10 kbars). The
deviatoric stress may affect mineral stability and generate mineral phase changes
(leading to slightly higher densities), as suggested in the gravity models of the
Sargodha high (figures 6 and 7).

Another area where bending stress is large enough to cause rupture of the
crustal rocks is the Hazara low seismic zone (HLZ, figures 2, 7 and 9). The large
negative bending moment occurring in the vicinity of the MMT produces a sharp
curvature of the Indian plate between km marks 0 and +100 km. It develops a
compressional deviatoric stress whose absolute value at km mark+40 is :
$| \sigma_x | = |[12 \times (-4.0 \times 10^{23} \times 0.8 \times 10^{-7}) \times 30 \times 10^3 /2]/(30 \times 10^3)^3 |$
$= 0.21 \times 10^9$ N/m^2 = 2.1 kbars, when taking the curvature of the least square curve.
In the case of the computed deflection, the deviatoric stress at km mark 40 is
$| \sigma_x | = 4.2$ kbars, twice as much. This flexural stress in large enough to induce
crustal failure (see figure 3 of Bird, 1978). Again seismicity studies carried out by
Seeber and Armbruster (1979) have demonstrated high seismic activity in the HLZ.
Fault plane solutions tend to suggest that the seismicity pattern is the result of incipient

reverse faulting in this region. The combination of the negative bending moment, as suggested by flexural modeling, and the northward motion of the buoyant Indian plate allow development of a stress-strain regime, which in the HLZ and Indus-Kohistan Seismic Zone (IKSZ) is expressed through initiation of crustal scale thrust faulting, producing the high seismic activity (see figure 9 of Seeber and Armbruster, 1979).

Finally, concerning the misfit between the flexure model and gravity model solutions, an improvement could be made by using a variable flexural rigidity with a linear variation of about 4.0×10^{23} Nm from the MMT to about 2.0×10^{23} Nm at the Sargodha ridge. However, since there is certainly an important contribution of the central Himalaya to the Sargodha ridge, there is no sense in trying to fit perfectly the constraints with a 2-dimensional model; this would require a 3-dimensional analysis. Because the plate is also bent towards the northeast due to the load of the central Himalaya, this adds some stiffness to the elastic plate and prevents the flexural bulge from freely migrating to the south, as computed by the 2-dimentional flexural model (figure 10).

SYNTHESIS - CONCLUSIONS

Available Bouguer gravity anomaly data from the Himalayan foreland of Pakistan are reinterpreted in an attempt to refine previous interpretations (Marussi, 1976; Farah et al., 1977) of the gross-structure of this region. Seismic reflection, surface geology and well data incorporated with the gravity data allow modeling of densities along a N-S profile extending from the MMT to south of the Sargodha ridge (figure 7). The gravity anomalies over the Pakistan fold and thrust belt show large deviations from Airy isostratic equilibrium (Marussi, 1976; figure 11). These deviations can be explained if we consider that the mass distribution is the sole consequence of the underthrusting of the Himalaya by a strong plate. The strength of the Indian plate partly supports the weight of the mountains and distributes the effect of this end load by flexing down in front of the Himalaya to form a basin (e.g., Karner and Watts, 1983; Lyon-Caen and Molnar, 1983). The resulting foredeep is in turn filled by sediment, the Siwalik group, eroded off the Himalaya. A more diffuse expression of the flexure of the underthrusting Indian plate is the creation of an outer "topographic rise", similar to the flexural bulge encountered at oceanic trenches (Molnar et al., 1976). In the foreland of Pakistan the Sargodha ridge seems to be the expression of such a flexural bulge (Yeats and Lawrence, 1984).

In northern Pakistan an excess of mass characterizes the Kohistan arc, whereas the foredeep basin between the MMT and the Salt Range shows a prominent deficit of mass. Finally, to the south, the Sargodha Ridge seems to be underlain by an excess of mass (figure 11). Modeling of the Bouguer gravity anomaly from the Sargodha high to the MMT shows that most of the gravity gradient is due to the shape of the Moho interface, except in the Sargodha ridge area where an anomalous excess of mass (about 1/3 of Bouguer anomaly contribution) resides in the lower crust due to flexural stress. After bulging up beneath the Sargodha high, the Moho dips gently northward at roughly 2°, flattens out north of the Peshawar basin (figures 7 and 11), and slopes gently southward (less than 2°) towards the MMT. To the north of the MMT, the Moho seems to drop dramatically and probably reaches a depth of at least 60 to 65 km beneath the northern part of the Kohistan arc (figures 3 and 11).
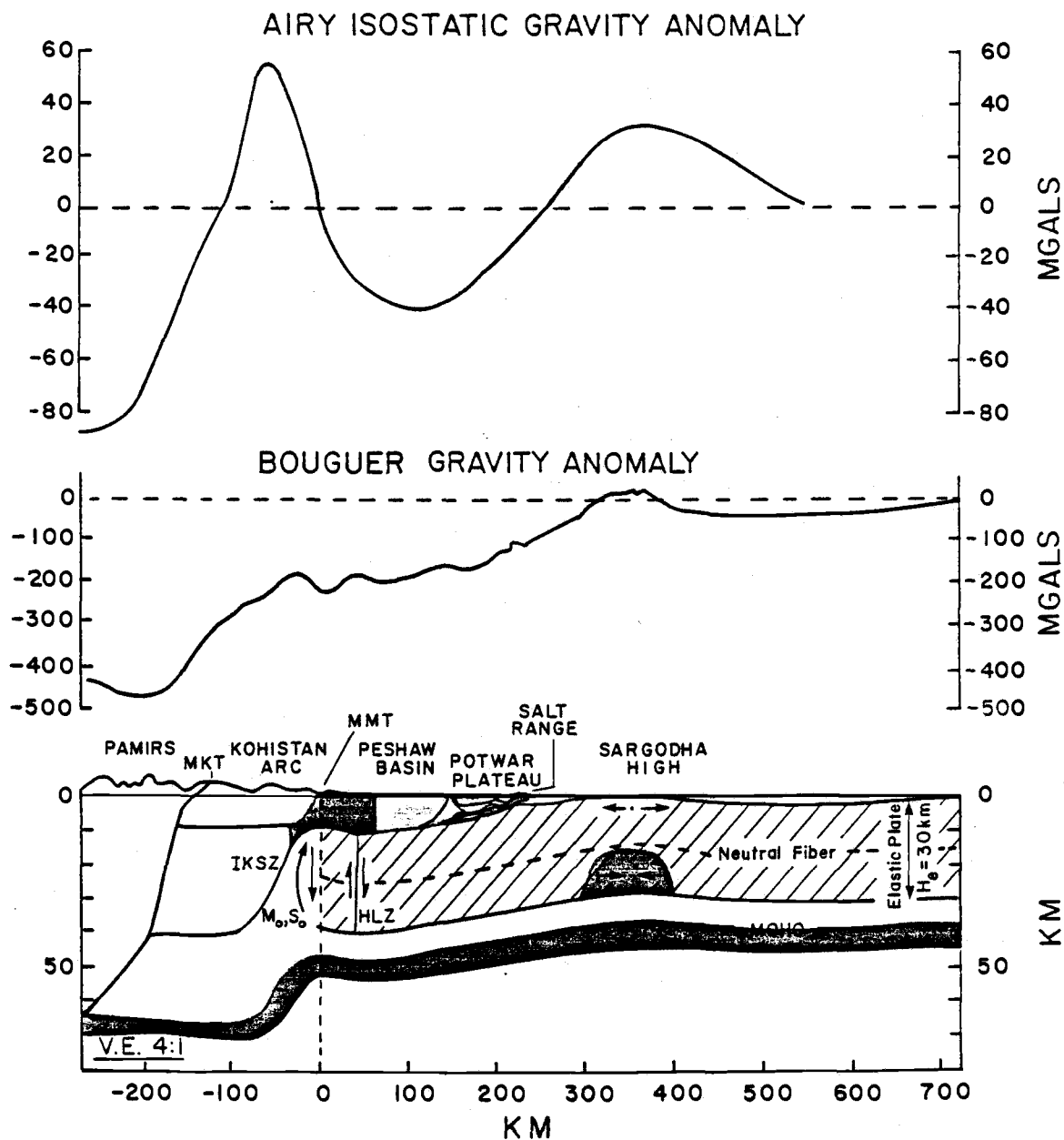
Figure 11 - Synthesis of the gravity and flexural analysis in the fold and thrust belt of Pakistan along cross section FF' (figures 2 and 3). Airy isostatic anomaly from Marussi (1976) assumed that: Normal thickness of the crust T = 30 km, density of the crust ρ_c = 2.67 gm/cm^3, and density of the upper mantle ρ_m = 3.3 gm/cm^3.

Investigations of the gravity field in this area currently undertaken by Malinconico and Adams (1986), will allow better understanding of the crustal structure north of the MMT. The second contribution to the Bouguer gravity anomaly observed between the MMT and the Sargodha ridge is the deepening of the sedimentary basin and the general northward density increase of the overthrust wedge. Short-wavelength components in the gravity field are the result of various geologic structures within the overthrust wedge (Lillie et al., in press; Baker, in prep.; Leathers, in prep.; Pennock, in prep.). The mechanics of the structures, such as the "triangle zone" of the northern Potwar Plateau and the Salt Range, are mainly governed by the abundance or paucity of an evaporite layer which acts as a decollement zone decoupling the crystalline basement of the Indian plate from the overthrust wedge (Jaumé, 1986; Jaumé and Lillie, in review). Also, basement faults attributed to lithospheric flexure contribute to some extent to the short-wavelength component of the gravity field of the Pakistan foreland.

In the second stage of this study the gravity anomalies were analysed in terms of the simple model of an elastic plate (Indian subcontinent) overlying an inviscid fluid. Subsurface densities in the foreland of the Pakistan fold-and-thrust belt, as well as the interpreted shape of the basement surface, are used to constrain the flexural rigidity of the plate and the forces that deform it. The profile of the computed elastic deflection of the top of the Indian plate agrees with the depth of the basement surface inferred from gravity and seismic reflection data, within a few hundred meters. A relatively small flexural rigidity of the Indian plate was required to fit the gravity anomaly in northern Pakistan. Compared to the values encountered in the central and eastern Himalaya (Karner and Watts, 1983; Lyon-Caen and Molnar,1983,1985), it is smaller by a factor of 10. This decrease in the flexural rigidity going from SE to NW along the Himalaya is expressed in the gravity field and has also been mentioned by Lyon-Caen and Molnar (1983, 1985) and Karner and Watts (1983). It is still not clear if these variations can be attributed to variations in the geotherm of the Indian plate or to other factors. Because the flexural rigidity of the Indian plate can vary by a factor of ten along the Himalayan arc, the corresponding elastic thickness can change from 30 - 40 km in northern Pakistan to as much as 80 - 100 km in central and eastern India.

The consequence is that, unlike in India where the crust and some of the upper mantle form the elastic plate, in northern Pakistan the elastic portion of the lithosphere is confined to the crust (figure 11). This framework can be used to explain tectonic features such as the Sargodha Ridge and the HLZ. In the area of the flexural bulge (Sargodha Ridge) a compressive region is developed below the neutral fiber, with a maximum amplitude at the bottom of the elastic plate, within the lower crust. The deviatoric stress generated by this compression is large enough to induce phase change metamorphism and create an anomalous excess of mass whose signature is apparent in the gravity anomaly. In contrast, because of the large elastic thickness of the Indian plate in the central Himalaya, the compressional zone is deeper, somewhere within the upper mantle. The plate bends less sharply in India than in northern Pakistan, meaning that the excess of mass encountered in the Sargodha region might not be present in the central and eastern Himalaya. If it is present, this excess of mass might not show up distinctly on the gravity anomaly due to the great depth at which it occurs.

Besides being successful in explaining the mass distribution in the foreland of the Pakistan fold and thrust belt, the flexural model provides important information about the stress regime within the Indian plate. Despite its simplicity the elastic model succeeds in predicting where the concentration of stress may induce brittle failure. Two areas are particularly subject to large flexural stresses that exceed values that crustal rocks can support: the Sargodha - Sha Kot Ridge and the Hazara Low Seismic zone (HLZ). These areas are also seismically active (Seeber et al., 1979). Normal faulting of the crystalline basement occurs in the Salt range area and Sargodha ridge, which can be related to the large extensional stress (above the neutral fiber) created by the downbending of the Indian plate. It is very similar to extensional rupture of oceanic crust observed by Schweller and Kulm (1978) in the Chile Trench.

In the area of the MMT a large vertical shear stress is applied to account for the northern Kohistan load. The strong negative bending moment (figure 11) that puts the top of the Indian plate north of the Peshawar basin under compressional stress exceeds the strength of the crustal rocks. Due to the net northward motion of the Indian plate and to the buttress effect of the crustal rocks stacked beneath the Kohistan arc, a tremendous compressive stress is generated that is released through reverse

faulting in the HLZ. The nature of the bending moment and the forces interacting in the area of the MMT not only explain the bending of the Indian plate south of the MMT, but also offer a plausible scenario for crustal thickening beneath the Kohistan region. Because of the light density of the Indian plate, crustal shortening by folding and thrust faulting is more likely to occur than subduction of the majority of this material. The stress regime in the MMT area seems to be consistent with imbrication of the Indian crust through reverse faulting. The thick crust beneath the Kohistan arc is probably a result of such megathrusting which produced Indian plate slivers that have been stacked beneath the arc as the Indian plate continued its northward migration.

BIBLIOGRAPHY

Acharyya, S.K., and K.K. Ray, Hydrocarbon possibilities of concealed Mesozoic - Paleogene sediments below Himalayan nappes - Reappraisal, *Amer. Assoc. Petrol. Geol. Bull.*, 66, 57-70, 1982.

Baker, D. M., Balanced structural cross section of the central Salt Range and Potwar Plateau of Pakistan: Shortening and overthrust deformation associated with a salt decollement, M.S. thesis, Oregon State University, Corvallis, Oregon, in prep., 1986.

Bird, P., Initiation of Intracontinental subduction in the Himalaya, *J. Geophys. Res.*, 83, 4975-4987, 1978.

Choudhury, S.K., Gravity and crustal thickness in the Indo-Gangetic Plains and Himalayan region, India, *Geophys. J. Roy. Astr. Soc.*, 40, 441-452, 1975.

Conte, S.D., and C. de Boor, Elementary Numerical Analysis, McGraw-Hill, New York, 3rd Edition, 1980.

Crawford, A.R., The Salt Range, the Kashmir syntaxis and the Pamir arc, *Earth Planet. Sci. Lett.*, 22, 371-379, 1974.

Davies, R.G., and A.R. Crawford, Petrography and age of the rocks of Bulland Hill, Kirana Hills, Sarghoda District, West Pakistan, *Geol. Mag.*, 108, 235-246, 1971.

Dewey, J.F., and J.M. Bird, Mountain belts and the new global tectonics, *J. Geophys. Res.*, 75, 2625-2647, 1970.

Dewey, J.F., and K. Burke, Hot spots and continental breakup: some implications for collisional orogeny, *Geology*, 2, 57-60, 1974.

Farah, A., M. A. Mirza, M.A. Ahmad, and M.H. Butt, Gravity field of the buried shield in the Punjab Plain, Pakistan, *Geol. Soc. Amer. Bull.*, 88, 1147-1155, 1977.

Finetti, I., F. Giorgetti, and G. Poretti, The Pakistani segment of the DSS-profile Nanga Parbat-Karakul (1974-1975), *Bolletino di Geofisica Teorica ed Applicata*, 21, 159-171, 1979.

Gansser, A., Geology of the Himalayas, Wiley-Interscience, London, p. 289, 1964.

Gee, E.R., Tectonic problems of the Sub-Himalayan region of Pakistan, *Kashmir Jour. Geol.*, 1, 11-18, 1983.

Gerald, C.F., and P.O. Wheatley, Applied Numerical Analysis, Addison-Wesley Publishing Company, Reading, Mass., 3rd Edition, 579 pp., 1984.

Hart, P. J., Ed., The Earth's Crust and Upper Mantle, American Geophysical Union, Washington, D. C., pp. 641-642, 1969.

Hurlbut, C.S., Jr., Revisor, Dana's Manual of Mineralogy, John Wiley & Sons, Inc., New York, 17th Edition, 1966.

Jaumé, S.C., The mechanics of the Salt Range-Potwar Plateau: Pakistan, quantitative and qualitative aspects of a fold-and-thrust belt underlain by evaporites, M.S. thesis, Oregon State University, Corvallis, Oregon, 58 p., 1986.

Jaumé, S.C., and R.J. Lillie, Active Tectonics of the Salt Range-Potwar Plateau, Pakistan: Mechanics of a Fold-and-Thrust Belt Underlain by Evaporites, *Tectonics*, in review, 1986.

Johnson, G.D., N.M. Johnson, N.D. Opdyke, and R.A.K. Tahirkheli, Magnetic reversal stratigraphy and sedimentary tectonic history of the upper Siwalik Group, eastern Salt Range and southwestern Kashmir, in *Geodynamics of Pakistan*, edited by A. Farah and K. De Jong, Geol. Surv. Pakistan, 149-165, 1979.

Kahn, M.A., R. Ahmed, H.A. Raza, and A. Kemal, Geology of Petroleum in Kohat-Potwar Depression, Pakistan, *Amer. Assoc. Pet. Geol. Bull.*, 70, 396-414, 1986.

Kaila, K.L., Structure and seismotectonics of the Himalaya-Pamir Hindukush Region and the Indian Plate Boundary, in *Zagros - Hindu Kush - Himalaya Geodynamic Evolution*, H.K. Gupta and F.M. Delany, Eds., American Geophysical Union, Washington, D.C., Geological Society of America, Boulder, Colorado, pp. 272-293, 1981.

Kaila, K.L., Deep seismic sounding studies in India, *Geophys. Res. Bull.*, 20(3), 309-328, 1982.

Kaila, K.L., and V.G. Krishna, Upper mantle velocity structure in the Hindukush region, Monograph on 'The International Pamir-Himalayan Project', 1980.

Karner, G.D., M.S. Steckler, and J. A. Thorne, Long-term thermo-mechanical properties of the continental lithosphere, *Nature*, 304, 250-253, 1983.

Karner, G.D., A.B. Watts, Gravity anomalies and flexure of the lithosphere at mountain ranges, *J. Geophys. R.*, 88, 10449-10477, 1983.

Kazmi, A. H., and R. A. Rama, Tectonic map of Pakistan, Geol. Surv. Pakistan, Quetta, 1982.

Kempe, D.R.C., The petrology of the Warsak alkaline granites, Pakistan, and their relationship to other alkaline rocks of the region, *Geol. Mag.*, 110, 385-495, 1973.

Kono, M., Gravity anomalies in east Nepal and their implications to the crustal structure of the Himalayas, *Geophys. J. Roy. Astr. Soc.*, 39, 283-300, 1974.

Leathers, M., Balanced structural cross section of the western Salt Range and Potwar plateau: Deformation near the strike-slip terminus of an overthrust sheet, M.S. thesis, Oregon State University, Corvallis, Oregon, in prep., 1986.

LeFort, P., Himalayas: The collided range. Present knowledge of the continental arc, *Am. Jour. Sci.*, 275-A, 1-44, 1975.

Lillie, R.J. and M. Yousuf, Modern analogs for some midcrustal reflections observed beneath collisional mountain belts, in *Reflection Seismology: The Continental Crust*, Amer. Geoph. Un., Geodynamics Series, Vol. 14, edited by M. Barazangi and L. Brown, 55-65, 1986.

Lillie, R.J., G.D Johnson, M. Yousuf, A.S.H. Zamin, and R.S. Yeats., Structural development within the Himalayan foreland fold-and-thrust belt in northern Pakistan. In *Basins of Eastern Canada and Modern Analogs*, edited by C. Beaumont and A. Tankard, Can. Assoc. Petro. Geol. Spec. Vol., in press, 1986.

Lyon-Caen, H., and P. Molnar, Constraints on the structure of the Himalaya from gravity anomalies and a flexural model of the lithosphere, *J. Geophys. Res.*, 88, 8171-8191, 1983.

Lyon-Caen, H., and P. Molnar, Gravity anomalies, flexure of the Indian plate, and the structure, support and evolution of the Himalaya and Ganga Basin, *Tectonics*, 4, 513-538, 1985.

Malinconico, L.L., Jr., Structure of the Himalayan suture zone of Pakistan interpreted from gravity and magnetic data, Ph.D. thesis at Dartmouth college, 1982.

Malinconico, L.L., Jr., The structure of the Kohistan-arc terrane in northern Pakistan as inferred from gravity data, *Tectonophysics*, 124, 297-307, 1986.

Malinconico, L.L., Jr., and K. Adams, Lithospheric underthrusting in the western Himalaya inferred from gravity data, GSA Abstract, 1986.

Marussi, A., Geophysics of the Karakorum, Brill, Leiden, 1961.

Marussi, A., Introductory report on geophysics, *Geotettonica Delle Zone Orogeniche del Kashmir Himalaya Karakorum - Hindu Kush - Pamir*, Accademia Nazionale dei Lincei, Roma, vol. 21, pp. 15-25, 1976.

Mattauer, M., Sur le mécanisme de formation de la schistosité dans l'Himalaya, *Earth Plan. Sci. Lett.*, 28, 144-154, 1975.

McAdoo, D.C., J. G. Caldwell, and D.L. Turcotte, On the elastic-perfectly plastic bending of the lithosphere under generalized loading with application to the Kuril Trench, *Geophys. J. R. astr. Soc.*, 54, 11-26, 1978.

Menke, W.H., and K.H. Jacob, Seismicity patterns in Pakistan and northwestern India associated with continental collision, *Seismol. Soc. America Bull.*, 66, 1695-1711, 1976.

Misch, P., Metasomatic granitization of Batholithic dimensions, *Am. Jour. of Sci*, 257, 204-245, 1949.

Mishra, D.C., Crustal structure and dynamics under Himalaya and Pamir ranges, *Earth and Planet. Sci. Lett.*, 57, 415-420, 1982.

Molnar, P., W.P. Chen, T. J. Fitch, P. Tapponnier, W.E.K. Warsi, and F. T. Wu, Structure and tectonics of the Himalaya: a brief summary of relevant geophysical observations, *Colloques internationaux du C.N.R.S.*, No. 268 - Ecologie et Geologie de l'Himalaya, 269-294, 1976.

Nafe, J.E., and C.L. Drake, Society of Exploration Geophysicists, Annual Meeting, 1957, Unpublished paper. The graph referred to is published in R.E. Sheriff, Encyclopedic Dictionary of Exploration Geophysics, Society of Exploration Geophysicists, 2nd Ed., p. 164, 1984.

Ni, J., and M. Barazangi, Seismotectonics of the Himalayan collision zone: Geometry

of the underthrusting Indian plate beneath the Himalaya, *J. Geophys. Res.*, 89, 1147-1163, 1984.

Pennock, N., Balanced structural cross section of the eastern Potwar Plateau, Pakistan: Shortening and deformation at the edge of a salt basin, M.S. thesis, Oregon State University, Corvallis, Oregon, in prep., 1986.

Powell, C.McA., and P.J. Conaghan, Plate tectonics and the Himalayas, *Earth and Planet. Sci. Lett.*, 20, 1-12, 1973.

Qureshy, M.N., Thickening of a basalt layer as a possible cause for the uplift of the Himalayas - a suggestion based on gravity data, *Tectonophys.*, 7, 137-157, 1969.

Qureshy, M.N., S.V. Venkatachalam and C. Subrahmanyam, Vertical tectonics in Middle Himalayas: an appraisal from recent gravity data, *Bull. Geol. Soc. Amer.*, 85, 921-926, 1974.

Raiverman, V., S.V. Kunte, and A. Mukherjea, Basin geometry, Cenozoic sedimentation and hydrocarbon prospects in northwestern Himalaya and Indo-Gangetic plains, *Petrol. Asia Jour.*, 6, 67-92, 1983.

Raynolds, R.G., and G.D. Johnson, Rates of Neogene depositional and deformational processes, northwest Himalayan foredeep margin, Pakistan, in *Geochronology and the Geological Record*, Geol. Soc. London, Spec. Stud., Vol. 17, in press, 1985.

Ritsema, A.R., K. Aki, P.J. Hart, and L. Knopoff, Eds., The Upper Mantle, Developments in Geotectonics 4, Elsevier Publishing Company, New York, pp. 143-145, 1972.

Roecker, S.W., Velocity structure of the Pamir-Hindu Kush region: Possible evidence of subducted crust, *J. Geophys. Research*, 87, 945-959, 1982.

Schweller, W.J., and L.D. Kulm, Extensional rupture of oceanic crust in the Chile trench, *Marine Geology*, 28, 271-291, 1978.

Seeber, L., J.G. Armbruster and R.C. Quittmeyer, Seismicity and continental subduction in the Himalayan arc; in *Zagros Hindu Kush, Himalaya Geodynamic evolution*, edited by Guptra and Delany, A.G.U. , Geodynamic series, 3, 215-242, 1981.

Seeber, L., J.G. Armbruster, Seismicity of the Hazara arc in northern Pakistan: Décollement versus basement faulting; in *Geodynamic of Pakistan* edited by Abul Farah and Kees A. Dejong, Geological Survey of Pakistan, 131-142, 1979.

Segawa, J., and Y. Tomoda, Gravity measurements near Japan and study of the upper mantle beneath the oceanic trench-marginal sea transition zones; in *Geophysical Monograph 19*, the Woolard volume edited by George H. Sutton, Murli H. Mangnani, and Ralph Moberly, A.G.U., 35-52, 1976.

Sheriff, R.E., Encyclopedic Dictionary of Exploration Geophysics, Society of Exploration Geophysicists, Tulsa, OK, 2nd. Ed., 323 pp., 1984.

Tahirkheli, R.A.K., M. Mattauer, F. Proust, and P. Tapponnier, The India-Eurasia suture zone in Northern Pakistan: synthesis and interpretation of recent data at plate scale, in *Geodynamics of Pakistan*, edited by A. Farah and K.A. DeJong, Geological Survey of Pakistan, pp. 125-130, 1979.

Talwani, M., J. L. Worzel, and M. Landisman, Rapid gravity computations for two-dimensional bodies with application to the Mendocino submarine fracture zone, *J. Geophys. Res.*, 64, 49-59, 1959.

Turcotte, D.L., and G. Schubert, Geodynamics: Applications of Continuum Physics to Geological Problems, John Wiley & Sons, New York, 450 pp., 1982.

Wang, C., and Y. Shi, On the tectonics of the Himalaya and the Tibet Plateau, *J. Geophys. Res.*, 87, 2949-2957. 1982.

Warsi, W.E.K.,and P. Molnar, Plate tectonics and gravity anomalies in India and the Himalaya, *Colloques Internationaux du Centre National de la Recherche Scientifique*, Himalaya: Sciences de la Terre, no. 268, 463-473, 1977.

Windley, B.F., Metamorphism and tectonics of the Himalaya, *Journal of the Geological Society of London*, 140, 849-865, 1983.

Woollard, G.P., Regional variations in gravity, in *The Earth's Crust and Upper Mantle*, Am. Geophys. Union Geophys. Mon. 13, edited by P.J. Hart, pp. 320-341, 1969.

Worzel, J.L., and G.L. Shurbet, Gravity interpretations from standard oceanic and continental crustal sections, *Geol. Soc. America*, Special Paper 62, 87-100,

1955.

Yeats, R.S., and A. Hussain, Timing of structural events in the Himalayan foothills of northwestern Pakistan, in prep., 1986.

Yeats, R.S., S.H. Khan, and M. Akhtar, Late Quaternary deformation of the Salt Range of Pakistan, *Geol. Soc. Amer. Bull.*, 95, 958-966, 1984.

Yeats, R.S., and R.D. Lawrence, Tectonics of the Himalayan thrust belt in northern Pakistan, in *Marine Geology and Oceanography of Arabian Sea and Coastal Pakistan*, edited by B.U. Haq and J.D. Milliman, 177-198, 1984.

APPENDICES

APPENDIX 1 :   SOLUTION OF THE " BIHARMONIC EQUATION "

Biharmonic equation (Turcotte and Schubert, 1982):

$$D \; \frac{\partial^4 W(x)}{\partial x^4} \; + \; g \, \Delta\rho(x) \, W(x) \; = \; Q(x) \tag{A-1}$$

The general analytic solution of the biharmonic equation in domains 4 and 5, and for the homogeneous case associated with (A-1) in domains 1, 2 and 3, is of the form (Turcotte and Schubert, 1982; Lyon-Caen and Molnar, 1983):

$$\begin{aligned} W_i(x) \; = \; & e^{x/\alpha_i} \, [\, A_i \cos (x/\alpha_i) + B_i \sin (x/\alpha_i)] \\ & + e^{-x/\alpha_i} \, [\, C_i \cos (x/\alpha_i) + D_i \sin (x/\alpha_i)] \end{aligned} \tag{A-2}$$

where:

$$\alpha_i = (\, 4 \, D \, / \, g \, \Delta\rho_i \,)^{1/4} \; ; \; i=1,5$$

The addition of a particular solution to the previous general solution is required to solve (A-1) in domains 1, 2 and 3. This can be done numerically by taking Fourier transforms of both sides of equation (A-1). Equation (A-2) has an oscillatory part (sines and cosines) with wave number α_i^{-1} (wavelength $2 \, \pi \, \alpha_i \approx \lambda_i$), and an exponential part with decay constant α_i. Concerning A_i , B_i , C_i , D_i , with i = 1 to 5, these are constants to be determined by boundary conditions. Once the boundary conditions have been specified, equation (A-1) describes the equilibrium of a system of forces and moments. A requirement in the solution of the biharmonic equation is that at the transition between each domain, there must be continuity of the deflection w(x) of the plate, of the slope $\partial W/\partial x$, of the bending moment $M = - D \, (\, \partial^2 W/\partial x^2 \,)$, and of the vertical shear stress $S = - D \, (\, \partial^3 W/\partial x^3 \,)$. Also, the bending moment M_0 and vertical shear stress S_0 must be specified at X_0, and the slope $\partial W/\partial x$ and

deflection W must be specified at X_{end} (figure 8).

Instead of using a "semi-analytical method" as in the flexural models of Lyon-Caen andMolnar (1983, 1984, and 1985) in the central Himalaya, a numerical method based on finite difference approximation is used to solve the biharmonic equation .

First of all, the Indian plate is divided into N = 500 intervals. We want to determine the deflection W at N+1 points along the x axis. The problem amounts to solving the equation :

$$\nabla^4 W = (Q(x) - g \, \Delta\rho(x) \, W(x)) / D = F(x) \qquad (A\text{-}3)$$

where:

∇^4 = biharmonic operator (fourth derivative of W (x)).

W (x) = deflection of the plate at abscissa x.

Q (x) = topographic load acting on the plate at x.

$\Delta\rho(x)$ = density contrast between the 2 materials above and below the plate.

F (x) = function representint the biharmonic operator.

g = gravitational attraction .

D = flexural rigidity of the plate.

The finite difference approximation of (A-3) is (Gerald and Whiley, 1984):

$$(W_{i+2} + 4W_{i+1} + 6W_i - 4W_{i-1} + W_{i-2}) / (\Delta x)^4 = (Q_i - g \, \Delta\rho_i \, W_i) / D = F_i \qquad (A\text{-}4)$$

where:

W_i = i [th] finite value of W, (i =2, N-2 where N is the number of intervals used in the finite difference method).

F_i = i [th] finite value of F (i = 2, N-2).

Δx = step size between 2 points (Δx = h = length of one interval).

$\Delta\rho_i$ = i [th] finite value of the density contrast between material above and beneath the plate (i = 2, N -2).

Q_i = i^{th} finite value of the load Q (i = 2, N-2).

g   =   gravitational attraction.

D   =   flexural rigidity of the plate.

Equation (A-4) can be rewritten as :

$$DW_{i-2}/h^4 - 4DW_{i-1}/h^4 + (6D/h^4 + g\Delta\rho_i)W_i - 4DW_{i+1}/h^4 + DW_{i+2}/h^4 = Q_i \quad (A-5)$$

In addition, one needs to define the boundary conditions (figures 8 and A). At $x = X_0$ = 0 km the bending moment $M_0 = -D \, (\partial^2 w/\partial x^2)$, and the vertical shear stress $S_0 = -D \, (\partial^3 w/\partial x^3)$ are specified. The deflection W_0 and the slope $\partial W/\partial x$ are still unknown. At $x = X_{end} = 1000$ km (approximation of $+\infty$), the deflection of the plate and its slope must be 0.

The bending moment M_0, shear stress S_0 and slope can be approximated by finite differences:

* Bending moment M_0 at X_0:

$$-DW_0/h^2 + 2DW_1/h^2 - DW_2/h^2 = M_0$$

* Vertical shear stress S_0 at X_0:

$$DW_0/h^3 - 3DW_1/h^3 + 3DW_2/h^3 - DW_3/h^3 = S_0$$

* Slope at X_{end}:

$$-W_{N-1}/h + W_N/h = slope$$

Incorporating the boundary conditions with the finite difference approximation of the biharmonic operator (A-5) leads to the system of N+1 = NP1 = 501 equations.

BOUNDARY CONDITIONS:

X = 0   X = + inf.

W(x) ?
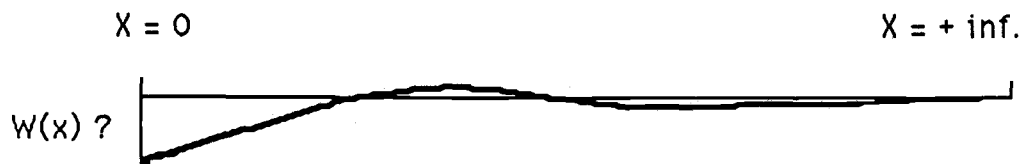
Specify:

* Bending moment (M_0)   * No deflection

* vertical shear stress (S_0)   * No slope

Figure A - Boundary conditions required to solve the biharmonic equation.

Equation 1:

$$-DW_0/h^2 + 2DW_1/h^2 - DW_2/h^2 = M_0$$

Equation 2:

$$DW_0/h^3 - 3DW_1/h^3 + 3DW_2/h^3 - DW_3/h^3 = S_0$$

Equations 3 to N-1:

$$DW_0/h^4 - 4DW_1/h^4 + (6D/h^4 + g\Delta\rho_2)W_2 - 4DW_3/h^3 + DW_4/h^4 = Q_2$$
$$DW_1/h^4 - 4DW_2/h^4 + (6D/h^4 + g\Delta\rho_3)W_3 - 4DW_4/h^3 + DW_5/h^4 = Q_3$$

$$DW_{N-4}/h^4 - 4DW_{N-3}/h^4 + (6D/h^4 + g\Delta\rho_{N-2})W_{N-2} - 4DW_{N-1}/h^3 + DW_N/h^4 = Q_{N-2}$$

Equation N:

$$- W_{N-1}/h + W_N/h = slope$$

Equation N+1:

$$W_N = W_{end}$$

Putting the system of equation in matrix form amounts to solving the problem A*W = B.

$$
\underset{A}{\begin{pmatrix}
-D/h^2 & 2D/h^2 & -D/h^2 & 0 & \cdots\cdots\cdots\cdots\cdots\cdots\cdots\cdots & & & 0 \\
D/h^3 & -3D/h^3 & 3D/h^3 & -D/h^3 & 0 \cdots\cdots\cdots\cdots\cdots\cdots & & & 0 \\
D/h^4 & -4D/h^4 & 6D/h^4+g\Delta\rho_2 & -4D/h^4 & D/h^4 & 0 \cdots\cdots\cdots & & 0 \\
0 & D/h^4 & -4D/h^4 & 6D/h^4+g\Delta\rho_3 & -4D/h^4 & D/h^4 & 0 \cdots & 0 \\
& \cdot & \cdot & \cdot & \cdot & \cdot & \cdot & \\
0 \cdots\cdots\cdots 0 & D/h^4 & -4D/h^4 & 6D/h^4+g\Delta\rho_{N-2} & -4D/h^4 & D/h^4 \\
0 \cdots\cdots\cdots\cdots\cdots\cdots\cdots\cdots\cdots\cdots 0 & & & & -1/h & 1/h \\
0 \cdots\cdots\cdots\cdots\cdots\cdots\cdots\cdots\cdots\cdots\cdots\cdots 0 & & & & & 1
\end{pmatrix}}
\underset{W}{\begin{pmatrix}
W_0 \\ W_1 \\ W_2 \\ W_3 \\ \cdot \\ W_{N-2} \\ W_{N-1} \\ W_N
\end{pmatrix}}
=
\underset{B}{\begin{pmatrix}
M_0 \\ S_0 \\ Q_2 \\ Q_3 \\ \cdot \\ Q_{N-2} \\ \text{Slope} \\ W_{end}
\end{pmatrix}}
$$

A is a (NP1xNP1) quintadiagonal coefficient matrix, while B is the known right hand side vector containing the boundary conditions and the topographic load values. W is the vector for the unknown solution of the deflection of the Indian plate.

Because of the degree of symetry and the sparseness of the quintadiagonal matrix A, one can reduce matrix A to 5 vectors containing the diagonal elements. This allows you to save a lot of computer storage. The matrix equation A*W = B is then solved by subroutine " FSOL " through main program " FLEXDUR ", as described in Appendix 2.

APPENDIX 2.   COMPUTER PROGRAMS :

FLEXDUR

```
C  Program FLEXDUR                                    October 1986.
C  Written in Fortran 5, on Data General " Eclipse C-150 "
C  by:   Yannick DUROY
C        Geophysics group
C        College of Oceanography
C        Oregon State University
C        Corvallis, Or 97331, USA.
C  ----------------------------------------------------------------------
C
C        This Fortran program is designed to perform two-dimensional flexural
C  modeling.  The model is one of a thin elastic plate overlaying an inviscid fluid.  The
C  plate is subject to a static load and to some external forces.  The deflection of such a
C  plate is governed by the " biharmonic equation " ( Turcotte and Schubert, 1982) :
C
C            D*(∂⁴W(x)/∂x⁴)  +  g*DELTARO(x)*W(x)  =   Q(x)
C
C        A finite difference approximation method is used to solve the biharmonic
C  equation.
C        The problem is reduced to a matrix equation A*W = B   (A is a coefficient
C  matrix, B a known righthand side vector, W the unknown solution vector).  Once a
C  solution of the deflection is obtained it is compared to the solution of the shape of
C  the plate as interpreted from gravity modeling.
C        The topographic load data and gravity derived shape of the plate data should
C  be input via an input file.
C        The program allows to input five blocks (B1, B2, B3, B4, B5) with different
C  densities, above the plate.  Block (B6) is given a density representing the viscous
C  fluid beneath the plate.
```

C   A bending moment M_0 and a shear stress S_0 can be applied at the end of the
C plate (at X = 0 km). At X = H*NP1 = 1000 km, one needs to specify the slope
C and deflection values of the elastic plate (H = step size, in this particular case it is
C taken as 2 km, NP1 = 500 and can be increased depending on the computer storage
C capacity).
C
C   Note : Program "FLEXDUR" requires the use of subroutine "FSOL".
C
C --
C
C   PARAMETERS :
C
C   Q   - Array containing the input topographic load data,
C   (input values must be in N/km^2).
C   DELTRO   - Array containing density contrast values (kg/km^3)
C   WGRAV   - Array containing values of the shape of the plate
C   interpreted from gravity model (km).
C   VA, VB, VC - Arrays containing the diagonal elements of the
C   VD, VE   quintadiagonal coefficient matrix A in the finite
C   difference approximation.
C   B   - Righthand side vector containing topographic load data
C   and boundary conditions. To be declared in a
C   COMMON statement to save space when the vector is
C   transferred to subroutine "FSOL".
C   W   - Solution vector for the deflection of the elastic plate.
C   Output values are in km. Also to be declared in a
C   COMMON statement.
C   ROB1,ROB2- Densities of blocks above and beneath the plate (input
C   ROB3,ROB4 in g/cm^3).
C   ROB5,ROB6
C   D   - Flexural rigidity of the plate (input in N.m).

```
C              AM0        -   Bending moment applied at the end of the plate (input
C                             in N).  It is considered positive for downward
C                             bending.
C              S0         -   Vertical shear stress applied at the end of the plate
C                             (input in N/m).  Positive downward.
C
C       Note :  Dimensions of the arrays as well as the step size in the finite difference
C               approximation can be redefined to fit computer storage capacity or
C               needs of the user.
C
C  ----------------------------------------------------------------------------------
C
C       DATA :
C
C              H          -   Step size in the finite difference approximation,
C                             (in km).
C              G          -   Gravitational attraction, (m/sec²).
C              WEND       -   End condition for the deflection of the plate.
C              SLOPE      -   End condition for the slope of the plate.
C              EPSI       -   In subroutine "FSOL" for testing by division by near
C                             zero numbers.  If a number is close to or equal to zero,
C                             an error message will appear.
C              IFIRST     -   In subroutine "FSOL", set IFIRST = 0 if on the first
C                             call to the subroutine, and IFIRST = 1 If any
C                             subsequent calls.
C              NP2, NP1   -   Indexes decreasing by 1 from NP2.
C              N, NM1         NP2 being the maximum dimension of the arrays.
C              IBB1, IEB1 -   Index of beginning of block 1, index of end of block
C              IBB2, IEB2     1, index of beginning of block 2, etc ...  They are
C              IBB3,IEB3      function  of the step size.  IBB1 = 1, IEB5 = NP2.
C              IBB4, IEB4
```

```
C            IBB5, IEB5
C            LUI1, LUI2  -   Output and input logical numbers.
C            LUO
C
C -----------------------------------------------------------------------------------------
C
      DIMENSION Q (501), DELTRO (501), WGRAV (501)
      DIMENSION VA (2), VB (3), VC (501), VD (4), VE (3)

      DIMENSION B (501), W (501)
      COMMON/BLK2/B,W

C
C -----   Input data
C

      DATA G/9.8/,EPSI/1.0E-10/,IFIRST/0/
      DATA H/2.0/,SLOPE/0.0/,WEND/0.0/
      DATA N/499/,NM1/498/,NP1/500/,NP2/501/
      DATA IBB1/1/,IEB1/30/,IBB2/31/,IEB2/75/,IBB3/76/,IEB3/119/,
     *      IBB4/120/,IEB4/175/,IBB5/176/,IEB5/501/
      DATA LUI1/1/,LUI2/2/,LUO/3/

C
C -----   Open input and output files
C

      TYPE 'Enter name of the file containing shape of the plate data from gravity !'
      CALL INFILE(LUI1)

      TYPE 'Enter name of the file containing the topographic load data !'
```

```
      CALL INFILE(LUI2)

      TYPE 'Enter name of the output file !'
      CALL OUTFILE(LUO)
C
C -----    Input flexural model variables
C


      ACCEPT 'Density of first block (B1) above plate (g/cm^3) ? ',ROB1
      ACCEPT 'Density of second block (B2) above plate (g/cm^3) ? ',ROB2
      ACCEPT 'Density of third block (B3) above plate (g/cm^3) ? ',ROB3
      ACCEPT 'Density of fourth block (B4) above plate (g/cm^3) ? ',ROB4
      ACCEPT 'Density of fifth block (B5) above plate (g/cm^3) ? ',ROB5
      ACCEPT 'Density of material beneath elastic plate (g/cm^3) ? ',ROB6
      ACCEPT 'Input flexural rigidity !  D = ? (N.m) ', D
      ACCEPT 'Applied bending moment at X_0;  M_0 = ? (N) ',AM0
      ACCEPT 'Applied vertical shear stress at X_0;  S0 = ? (N/m) ',S0


C
C -----    Redefine units of variables for consistency in computation.
C


      ROB1=ROB1*1.E 12
      ROB2=ROB2*1.E 12
      ROB3=ROB3*1.E 12
      ROB4=ROB4*1.E 12
      ROB5=ROB5*1.E 12
      ROB6=ROB6*1.E 12
      D=D*1.E-03
      S0=S0*1.E 03
```

```
C
C -----   Read shape of the plate data derived from gravity modeling
C -----   and initialize variable arrays.
C

      DO 10 I=1,NP2
      READ(LUI1,100) WGRAV(I)
100 FORMAT(E17.9)
      DELTRO(I)=0.0
      W(I)=0.0
      B(I)=0.0
  10  CONTINUE


C
C -----   Read topographic load data
C

      DO 20 I=1,NP2
      READ(LUI2,101) Q(I)
101  FORMAT(E17.9)
20   CONTINUE


C
C -----   Compute density contrasts between blocks above and beneath the plate.
C

      DO 30 I=IBB1,IEB1
      DELTRO(I)=ROB6-ROB1
30   CONTINUE

      DO 35 I=IBB2,IEB2
```

```
      DELTRO(I)=ROB6-ROB2
35    CONTINUE

      DO 40 I=IBB3,IEB3
      DELTRO(I)=ROB6-ROB3
40    CONTINUE

      DO 45 I=IBB4,IEB4
      DELTRO(I)=ROB6-ROB4
45    CONTINUE

      DO 50 I=IBB5,IEB5
      DELTRO(I)=ROB6-ROB5
50    CONTINUE

C
C -----   Compute elements of the five vectors representing
C -----   the quintadiagonal coefficient matrix A.
C

      VA(1)=D/(H*H*H*H)
      VA(2)=0.0

      VB(1)=D/(H*H*H)
      VB(2)=-4.0*D/(H*H*H*H)
      VB(3)=0.0

      VC(1)=-D/(H*H)
      VC(2)=-3.0*D/(H*H*H)
      DO 60 I=3,N
      VC(I)=6.0*D/(H*H*H*H)+G*DELTR0(I)
```

```
60    CONTINUE
      VC(NP1)=-1.0/H
      VC(NP2)=1.0

      VD(1)=2.0*D/(H*H)
      VD(2)=3.0*D/(H*H*H)
      VD(3)=-4.0*D/(H*H*H*H)
      VD(4)=1.0/H

      VE(1)=-D/(H*H)
      VE(2)=-D/(H*H*H)
      VE(3)=D/(H*H*H*H)


C
C -----    Load righthand side vector B with boundary conditions
C -----    and topographic load values.
C

      B(1)=AM0
      B(2)=S0
      DO 65 I=3,N
      B(I)=Q(I)
65    CONTINUE
      B(NP1)=SLOPE
      B(NP2)=WEND


C
C -----    Now we call subroutine "FSOL" for the solution of
C -----    the matrix problem A*W = B
C
```

```
      CALL FSOL(VA,VB,VC,VD,VE,NP2,EPSI,LUO,IFIRST)


C
C -----    Compare solution of the flexural model with solution from gravity model,
C -----    and compute the maximum difference and average difference between
C -----    the flexure and gravity solutions.
C


      DIFMAX=0.0
      DIFAV=0.0
      SUM=0.0


      DO 900 I=1,NP2
      SUM=SUM+ABS(W(I)-WGRAV(I))
      IF(ABS(W(I)-WGRAV(I)).GT.DIFMAX) GOTO 850
      GOTO 900
 850  DIFMAX=ABS(W(I)-WGRAV(I))
 900  CONTINUE


      DIFAV=SUM/FLOAT(NP2)


C
C -----    Write results to output file
C


 800  WRITE(LUO,300) AM0,WEND,S0*1.E-03,SLOPE,H,ROB1*1.E-12,
     *                ROB2*1.E-12,ROB3*1.E-12,ROB4*1.E-12,ROB5*1.E-12
     *                ROB6*1.E-12,D*1.E 03
 300  FORMAT(///,3X,'SOLUTION OF BIHARMONIC EQUATION : ',//,
     *    6X,'D*(∂⁴W(x)/∂x⁴) + g*DELTARO(x)*W(x) = Q(x) ',//,
     *    3X,'With the boundary conditions : ',//,
```

```
     *  6X,'x = 0km',15X,'x = 1000 km',/,
     *  6X,'M_0 = ',E9.3,' N ',6X,'W = ',E10.4,' km ',/,
     *  6X,'S_0 = ',E9.3,' N/m ',6X,' ∂W/∂x = ',E10.4,//,
     *  3X,'PARAMETERS :',//,6X,'Step size h = ',E8.1,' km ',/,
     *  6X,'Density of first block above plate = ',E9.3,' g/cm^3 ',/,
     *  6X,'Density of second block above plate = ',E9.3,' g/cm^3 ',/,
     *  6X,'Density of third block above plate = ',E9.3,' g/cm^3 ',/,
     *  6X,'Density of fourth block above plate = ',E9.3,' g/cm^3 ',/,
     *  6X,'Density of fifth block above plate = ',E9.3,' g/cm^3 ',/,
     *  6X,'Density of material beneath elastic plate = ',E9.3,' g/cm^3 ',/,
     *  6X,'Flexural rigidity :  D = ',E10.3,' N.m',///,
     * 3X,'DEFLECTION VALUES : ',//,6X,'x',20X,'W(x)',//)


       HORLOC=0.0


       DO 90 I=1,NP2
       WRITE(LUO,301) HORLOC,W(I)
       HORLOC=HORLOC+H
90     CONTINUE


301  FORMAT(4X,F6.1,9X,E17.9)


       WRITE(LUO,950) DIFMAX,DIFAV
950  FORMAT(//,6X,'Maximum difference FLEX-GRAV = ',E10.4,' km',/,
       *          6X,'Average difference FLEX-GRAV = ',E10.4,' km')
C
C -----   Close all opened files.
C
       CALL RESET
       STOP
       END
```

<u>FSOL</u>

```
C  Subroutine FSOL                              October 1986.
C  Written in Fortran 5, on Data General " Eclipse C-150 "
C  by:   Yannick DUROY
C        Geophysics group
C        College of Oceanography
C        Oregon State University
C        Corvallis, Or 97331, USA.
C  -----------------------------------------------------------------------
C
C        This subroutine solves the five diagonal matrix equation A*W = B,
C  representing the finite difference approximation of the biharmonic equation.  The
C  subroutine is adapted from an algorithm to solve quintadiagonal system, which is
C  given in Elementary Numerical Analysis (Conte and de Boor, 1980).
C
C  -----------------------------------------------------------------------
C
C        PARAMETERS :
C
C            VA, VB,VC  -   Arrays containing the diagonal elements of the
C            VD, VE         quintadiagonal coefficient matrix A.
C                           Because of the degree of symetry of the coefficient
C                           matrix these arrays can be adequately dimensioned :
C                           VA (2), VB (3),VC (501), VD (4), VE (3).  They are
C                           arranged as follows :
```

```
C
C      | VC(1)   VD(1)   VE(1)                                            |
C      | VB(1)   VC(2)   VD(2)   VE(2)                                    |
C      | VA(1)   VB(2)   VC(3)   VD(3)   VE(3)                            |
C      |         VA(1)   VB(2)   VC(4)   VD(3)   VE(3)                    |
C      |                                                                 |
C      |    .    .    .    .    .    .    .    .    .    .    .    .      |
C      |                                                                 |
C      |                         VA(1)   VB(2)   VC(N)   VD(3)   VE(3)    |
C      |                                 VA(2)   VB(3)   VC(NP1)  VD(4)   |
C      |                                         VA(2)    VB(3)  VC(NP2)  |
C
C      Note : The matrix should be arranged so that the vector VC is the largest of
C             the vectors,  if possible (i.e. The matrix is diagonally dominant).
C             Note in particular that VC (1) must be non-zero.
C
C             W          -  The vector of unknowns.
C             B          -  The constants on the righthand side of the equation
C                           (coefficient matrix A) * W = B.
C                           To save some memory space declare vectors W and B
C                           in a COMMON statement.
C             N          -  The length of all the vectors.  That is, there are
C                           N equations in N unknowns.  Presently N must be
C                           less than or equal to 501.  For larger N's,
C                           redimension the arrays DEL, OME, BET, and
C                           HVEC.
C             EPSI       -  For testing by division by near-zero numbers.  If a
```

```
C                              number is close to or equal to zero an error message
C                              will be printed.
C              LU           -  A logical unit number on which to write error
C                              messages.
C              IFIRST       -  This subroutine can solve many matrix equations all
C                              with the same matrix but each with different B's quite
C                              efficiently.  To do this, set IFIRST = 0 on the first
C                              call, and IFIRST = 1 on all subsequent calls having
C                              the same matrix.
C
C --------------------------------------------------------------------------------
C

      COMPILER DOUBLE PRECISION

      SUBROUTINE FSOL(VA,VB,VC,VD,VE,N,EPSI,LU,IFIRST)

      DIMENSION VA(2),VB(3),VC(501),VD(4),VE(3)
      DIMENSION DEL(501),OME(501),BET(501),HVEC(501)

      DIMENSION B(501),W(501)
      COMMON/BLK2/B,W

C
C -----   Compute intermediate result vectors if necessary.
C

      IF(IFIRST.NE.0) GOTO 100

      DEL(1)=0.0
```

```
C
C -----    Initialize first two locations of intermediate result arrays.
C

      OME(1)=VC(1)
      IF(ABS(OME(1)).LE.EPSI) GOTO 500
      BET(1)=VD(1)/OME(1)

      DEL(2)=VB(1)
      OME(2)=VC(2)-DEL(2)*BET(1)
      IF(ABS(OME(2)).LE.EPSI) GOTO 500
      BET(2)=(VD(2)-DEL(2)*VE(1)/OME(1)))/OME(2)

C
C -----    Recursively computes the other elements.
C

      DO 50 I=3,N-2
      IF(I.EQ.3) ECSTE1=VE(1)
      IF(I.EQ.4) ECSTE1=VE(2)
      IF(I.GT.4) ECSTE1=VE(3)
      DEL(I)=VB(2)-VA(1)*BET(I-2)
      OME(I)=VC(I)-VA(1)*(ECSTE1/OME(I-2))-DEL(I)*BET(I-1)
      IF(ABS(OME(I)).LE.EPSI) GOTO 500
      IF(I.EQ.3) ECSTE2=VE(2)
      IF(I.GT.3) ECSTE2=VE(3)
      BET(I)=(VD(3)-DEL(I)*(ECSTE2/OME(I-1)))/OME(I)
  50  CONTINUE

      DEL(N-1)=VB(3)-VA(2)*BET(N-3)
      OME(N-1)=VC(N-1)-VA(2)*(VE(3)/OME(N-3))-DEL(N-1)*BET(N-2)
```

```fortran
      IF(ABS(OME(N-1)).LE.EPSI) GOTO 500
      BET(N-1)=(VD(4)-DEL(N-1)*(VE(3)/OME(N-2)))/OME(N-1)

      DEL(N)=VB(3)-VA(2)*BET(N-2)
      OME(N)=VC(N)-VA(2)*(VE(3)/OME(N-2))-DEL(N)*BET(N-1)
      IF(ABS(OME(N)).LE.EPSI) GOTO 500
      BET(N)=0.0

C
C -----    Compute the intermediate result vector HVEC from B.
C

100   HVEC(1)=B(1)/OME(1)
      HVEC(2)=(B(2)-DEL(2)*HVEC(1))/OME(2)
      DO 150 I=3,N
      ACSTE=VA(1)
      IF(I.GT.N-2) ACSTE=VA(2)
      HVEC(I)=(B(I)-ACSTE*HVEC(I-2)-DEL(I)*HVEC(I-1))/0ME(I)
150   CONTINUE

C
C -----    Backsolve for solution.
C

      W(N)=HVEC(N)
      W(N-1)=HVEC(N-1)-BET(N-1)*W(N)
      DO 200 I=N-2,1,-1
      IF(I.EQ.1) ECSTE3=VE(1)
      IF(I.EQ.2) ECSTE3=VE(2)
      IF(I.GT.2) ECSTE3=VE(3)
      W(I)=HVEC(I)-BET(I)*W(I+1)-(ECSTE3/OME(I))*W(I+2)
```

```
200  CONTINUE

       GOTO 700


C
C -----    Error message.
C

500  WRITE(LU,600)
600  FORMAT('Warning from subroutine FSOL : ',
     *            'Division by near-zero number.')

700  RETURN
       END
```